 doi:10.20944/preprints202205.0057.v1

Article

Min-Max Regret-Based Approach for Sizing and Placement of DGs in Distribution System Under A 24h Load Horizon

Asad Abbas[1], Saeed Mian Qaisar[2,3], Asad Waqar[4,*], Nasim Ullah[5] and Ahmad Aziz Al Ahmadi[5*]

1 Department of Electrical Engineering, Chungnam National University, Daejeon, South Korea
2 College of Engineering, Effat University, 22332, Jeddah, Saudi Arabia; sqaisar@effatuniversity.edu.sa (S.M.Q)
3 Communication and Signal Processing Lab, Energy and Technology Center, Effat University, 22332, Jeddah, Saudi Arabia
4 Department of Electrical Engineering, Bahria University, 44000 Islamabad, Pakistan; asadwaqar.buic@bahria.edu.pk (A.W)
5 Department of Electrical Engineering, College of Engineering, Taif University, Taif 21944, Saudi Arabia, nasimullah@tu.edu.sa (N.U.); aziz@tu.edu.sa (A.A.A.-A)
* Correspondence: asadwaqar.buic@bahria.edu.pk (A.W); aziz@tu.edu.sa (A.A.A.-A)

Abstract: Load variations in any power system result in losses escalation and voltage drops. With the sensible and optimal allocation of distributed generators (DGs), these problems could be considerably mitigated. It has been seen in the priorly existing methods that ideally allocation of DGs has been carried out during fixed loads and constant power requirements. However, in real scenarios the loads are always variable and allocation of DGs must be done in accordance to the variations of the connected load. Therefore, the current paper addressed the aforementioned problem by distinctive optimal allocation of DGs for each variability of 24hour load horizon. However, the single exclusive solution is considered among all allocations of 24 hours. The min-max regret concept has been utilized in order to deal with such methodology. Altogether, 24 scenarios are analyzed wherein each scenario corresponds to a specific hour of the respective day. The optimal allocation of DGs in terms of their optimal sizing and placement has been carried out by using three algorithms including battle royal optimization (BRO), accelerated particle swarm optimization (APSO) and genetic algorithm (GA). The multi-objective optimization problem is evaluated on the basis of minimum value criterion of the multi-objective index (MO). MO comprises of active and reactive power losses and voltage deviation. Hence, in order to find robustness of proposed technique, Conseil international des grands réseaux electriques (CIGRE's) MV benchmark model incorporating 14 buses has been considerably used as a test network. In the end the results of three proposed algorithms have been compared.

Keywords: Distributed generators; Sizes and Locations of DGs; DGs' allocation; Power losses; Min-max regret Criteria; Battle royal optimization

1. Introduction

The invention of electricity and advancement in technology has brought remarkable betterment to mankind [1]. In the whole regime, transmission and distribution networks are the most significant operators. The distribution networks comprise a complex and engaged system. Therefore, the poor performance of the distribution networks may deprive the whole power system. One of the major hurdle to the performance marker of the distribution network is load variations over time. These load variations lead to varying active and reactive power losses and voltage drops [2]. One of the significant methods is the optimal deployment of DGs to minimize the power losses and improve the voltage drops

 doi:10.20944/preprints202205.0057.v1

in the distribution networks [3]. These DGs could be fossil fuel-based or renewable energy-based. Furthermore, the deployment of DGs in networks brings on to significant installment and operational costs [4]. Therefore, it has to be always done by employing standard optimization algorithms.

In the published literature, numerous researchers have reported the deployment of DGs in networks about certain objectives. In [5], the authors have investigated the deployment of DGs in several rounds using a plant propagation algorithm while minimized active power losses (APL) and reduced voltage drop. While the researchers in [6] improved voltage stability index (VSI) along with the above two objectives by utilizing a newly introduced cloud model-based symbiotic organism search algorithm for DGs deployment. However, [7] explored optimal DGs deployment after and before system reconfiguration. Technical constraints are followed in [8] for optimal allocation of DGs without its violation and a selective particle swarm optimization algorithm (SPSO) is utilized in the presence of a non-uniformly distributed pattern of load. The study [9] involved the chaotic artificial flora optimization-based technique for multiple test scenarios of optimal allocation of DGs and system reconfiguration. In [10], multiple load models are considered for obtaining the optimal size and location of DGs using the student psychology-based optimization (SPBO) algorithm. In [11], the researchers considered oppositional sine cosine muted differential evolution algorithm (O-SCMDEA) for optimal DG placement and analyzed objective functions separately as well as a combined objective function. Moreover, the study conducted in [12] used a novel algorithm for optimal deployment of DGs which is the combination of improved-grey-wolf-optimization and the PSO algorithm.

In [13], single and multiple DGs are optimally placed using whale Optimization Algorithm (WOA) for minimizing various objectives, moreover, the study also considered types of DGs. In [14], the effective placement of DGs is carried out using the optimal locator index and utilized the kalman filter algorithm to obtain the optimal sizes of the DGs. In [15], system losses are minimized by optimal placement of multiple DGs using analytical formula however, the effects of DGs, load level and many other factors are also analyzed. In [16], the size of the PV-based DG is optimized using the PSO. The study is focused on probabilistic PV generation under varying load models. 1n [17], single and multiple DGs are deployed with unity and optimal power factor using adaptive PSO and modified gravitational search algorithm (GSA) algorithm.

In [18], a wind turbine-based DG is optimally placed and sized in the presence of time varying load and renewable generation. In [19], optimal placement and sizing of DGs is considered to minimize losses and improve bus voltages along with total energy cost minimization with artificial bee colony (ABC) algorithm. Whereas in [20], sensitivity analysis of CIGRE's MV benchmark is accomplished while integrating large-scale renewable energy. In [21], invasive weed optimization algorithm (IWO) is utilized for optimal DGs allocation to check loss sensitivity factors under different kinds of loads. In [22], DGs are parameterized by using the PSO and genetic algorithm (GA). The study is conducted for different load models to minimize system sensitivity, losses, and bus voltage instability. In [23], capacitors are placed in addition to wind power-based DGs in the distribution system. The objectives are to minimize real and reactive power losses and gas emissions and to improve bus voltage profiles. Studies considered various scenarios which are based on combination of different numbers and sizes of capacitors and DGs.

In [24], multiple scenarios are investigated through adaptive shuffled frogs leaping algorithm (ASFLA) while scenarios are based on different combinations of network reconfiguration and DGs deployment. In [25], the optimal DG allocation is achieved by minimizing both technical and economical related objectives using the cuckoo search algorithm (CSA). The DG parameterization is investigated at various real and reactive load models. In [26], the system power losses are reduced by effectively positioning and sizing DGs and capacitors. It is carried out by using the dragonfly algorithm. Different scenarios are studied, while each scenario is the combination of different numbers and sizes of DGs and capacitors placed in the IEEE 33 bus system.

 doi:10.20944/preprints202205.0057.v1

From the above literature [5-26], the authors in published literature considered the allocation of DGs based on the static loads. Some of the authors evaluated the allocation of DGs for time-varying load while the location and size of DGs are calculated at average load. Moreover, some researchers considered multiple loads; however, each segregate allocation is achieved for a particular load instead of a single allocation for a combined load. People in the literature have obtained allocation for the probabilistic load and generation. Furthermore, most of them considered the static generation from renewable sources instead of time-varying generation. Certain studies investigate scenarios depending on the number and types of DGs and capacitors in the power system. However, they did not consider distinct loads and generations for each specific scenario.

The above points have analyzed that previous works utilized single-point analysis; however, in reality, electricity demand variates with different times of the day, resulting in losses variations at each specific duration. Hence, DG allocation at static particular load and generation (that may be any form, i.e., probabilistic generation/load) does not encounter the whole situation, and that's why DGs allocation for each time setting must be accomplished. Then the suitable allocation is to select among all allocations having desire objectives.

The main contributions of this paper are:

- The min-max regret criteria is analyzed and implemented for calculating the single robust optimal allocation of DGs among all optimal DGs' allocations of 24 scenarios. Although, this technique is used first time in these types of problems.
- Problem is formulated in scenarios such as each scenario representing a particular hour's load and generation.
- The methodology is implemented under the 24 hour varying load and renewable generation of wind and solar DGs.
- Battle royal optimization (BRO) algorithm is first time considered for DGs placement in the current study according to the best of the author's knowledge and also investigate performance and compared the results with APSA, and GA algorithm at individual and as well as combine objective value.
- Optimal allocation of DGs are obtained for each particular scenario by minimizing MO.
- Active power losses, reactive power losses, and buses voltage profiles are analyzed and discussed for each specific scenario.
- Energy losses of the whole day are calculated and discussed.

The above objectives clearly illustrate the system analysis at various times of the day and are thus beneficial in a way to get in touch with losses with varying demand. Hence, DGs allocations can be accomplished at each specific duration and, in turn, results in an optimal allocation of DGs for the whole day. The rest of the paper is organized as follows. In section 2 and 3, problem formulation and optimization algorithms are enlightened. Similarly, section 4 deals with the mathematical modeling of the optimization problem. Furthermore, in section 5 results and discussions are described. Lastly, section 6 concludes the paper.

2. Problem Formulation

The problem formulation involves the newton Raphson load flow (NRLF) and the findings associated with the optimal allocation of DGs using MO while considering various constraints. Optimal allocation of DGs means incursion of DGs in the system at an optimum point accompanied with optimal size and location. The system block diagram is illustrated in Figure 1. The first stage presents inputs of the system such as 24h load horizon (L), DG (/s) active and reactive power (P and Q), which have different values for each considered scenario. The second stage determines the optimal allocations of DGs for all scenarios based

Preprints (www.preprints.org) | NOT PEER-REVIEWED | Posted: 6 May 2022 doi:10.20944/preprints202205.0057.v1

on minimum MO. Finally, at the third stage, single DG (/s) allocation is selected among all DGs at stage 2 using the min-max regret criteria.

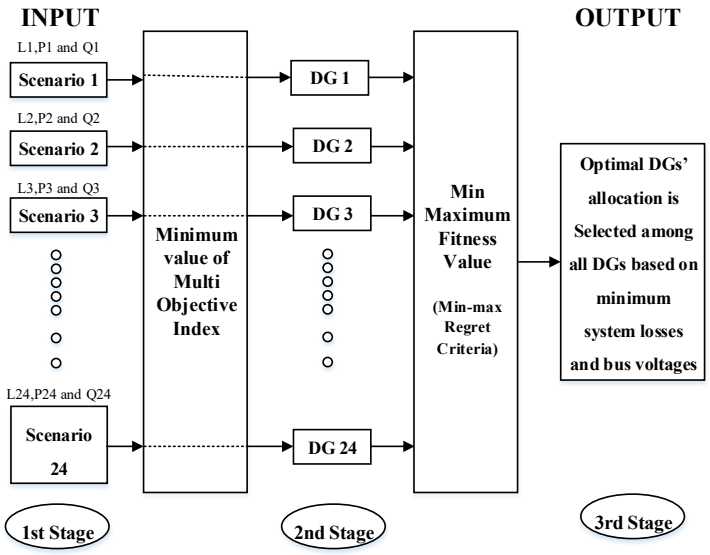

Figure 1. System Block Diagram

2.1. Load Flow Analysis

The load flow analysis (LFA) is an approach used to calculate bus voltage profiles and power flow across generators, loads, and branches under the static condition of a system [27]. It helps in the evaluation of system performance and therefore considered paramountly significant for the allocations of DGs. Different iterative methods such as fast-decoupled, Gauss-Seidel, and Newton-Raphson methods have been used for performing the LFA in literature. NRLF method converges faster as compared to the fast-decoupled and Gauss-Seidel approaches [28]. Following the study [5] for load flow analysis, the voltage across w^{th} bus of any system can be calculated by using Eq. (1).

$$\underline{V}_w = \frac{1}{\underline{Y}_{ww}}\left[\frac{(P_w - jQ_w)}{\underline{V}_w^*} - \sum_{\substack{w=1 \\ w\neq i}}^{Num} \underline{Y}_{wi}\underline{V}_i\right] \tag{1}$$

In Eq. (1), the phasor voltages of bus w and i are denoted by $\underline{V}_w$ and $\underline{V}_i$ respectively. $\underline{V}_w^*$ and V_w represents the phasor conjugate and magnitude of the w^{th} bus, respectively. The magnitudes of active power of bus w is represented by P_w, while in case of Eq. (2), magnitude of reactive power of bus w is represented by Q_w, Eq. (3). $\underline{Y}_{wi}$ represents the phasor Y-bus matrix between w^{th} and i^{th} bus, whereas $\underline{Y}_{ww}$ represents the phasor Y-bus matrix at the w^{th} bus.

$$P_w = \sum_{i=1}^{Num} Y_{wi}V_iV_w\cos(\theta_{wi} + \delta_i - \delta_w) \tag{2}$$

$$Q_w = -\sum_{i=1}^{Num} Y_{wi}V_iV_w\text{sine}(\theta_{wi} + \delta_i - \delta_w) \tag{3}$$

Active and reactive power across each bus can be calculated by using Eq. (2) and Eq. (3), respectively. Y_{wi} represents the magnitude of admittance between w^{th} and i^{th} bus. Num represents the total number of buses in the system. θ_{wi} refers to the angle of Y_{wi}. δ_i and δ_w are the voltage angle of bus i and w, respectively. The voltages calculated at each bus helps in the calculation of line currents of different branches by using Eq. (4).

Preprints (www.preprints.org) | NOT PEER-REVIEWED | Posted: 6 May 2022 doi:10.20944/preprints202205.0057.v1

$$\underline{I}_{wi} = \frac{\underline{V}_w - \underline{V}_i}{\underline{Z}_{wi}} \tag{4}$$

Wherein, the current and impedance of the branch between w^{th} and i^{th} bus are denoted by I_{wi} and Z_{wi}. The apparent powers at w and i bus can be calculated by using Eq. (5) and Eq. (6).

$$\underline{S}_w = \underline{V}_w \underline{I}_{wi}^* = P_w - jQ_w \tag{5}$$

$$\underline{S}_i = \underline{V}_i \underline{I}_{wi}^* = P_i - jQ_i \tag{6}$$

S_w and S_i represents the apparent complex power at w and i bus, respectively. Line losses between bus w and bus i are represented by $P_{loss\ wi}$, which can be calculated by using Eq. (7).

$$P_{loss\ wi} = P_w - P_i \tag{7}$$

2.2. Objective Function

The main objective function is to minimize the multi objective index.

2.2.1 Multi Objective Index

Multi objective index (MO) is the combination of active power loss index (API), reactive power loss index (RPI) and voltage deviation index (VD) [9]. The optimal allocation of DG can be achieved by minimizing the MO. The said applicable process is given by Eq. (8), whereas w1, w2, and w3 are weight indices of API, RPI, and VD, respectively [16]. API These indices are outlined in Table 1. It is basically the ultimate goal to minimize active and reactive power losses for a whole day while improving bus voltages profiles.

$$MO = w1 * API + w2 * RPI + w3 * VD \tag{8}$$

Table 1. Indices

Indices	W
API	0.5
RPI	0.25
VD	0.25

2.2.1.1 Active Power Loss Index

The system's active power loss is the first objective and can be calculated by using the total active power losses across each line. The process is given by Eq. (9) and Eq. (10), where, P_w and P_p are the active powers at bus w and p, respectively. The Line (L)$_{Aloss}$ is the active power loss at line L, whereas nl refers to the total number of lines in the system.

$$Line(L)_{A\,loss} = P_W - P_P \tag{9}$$

$$Total\ Active\ Power\ losses = \sum_{l=1}^{nl} Line(L)_{Aloss} \tag{10}$$

The *API* index is associated with the active power loss objective, which is the ratio of AP_{LDG} to AP_L. The process is given by Eq. (11), wherein, AP_{LDG} and AP_L are active power loss with and without DG, respectively.

$$API = [AP_{LDG} / AP_L] \tag{11}$$

2.2.1.2. Reactive Power Loss Index

The reactive power loss of the system is the second objective and can be calculated by using total reactive power losses across each line. The process is given by Eq. (12) and Eq. (13). Wherein, R_w and R_p are reactive powers across bus w and bus p respectively, while Line (L) $_{Rloss}$ is the reactive power loss at line L whereas nl tells the total number of lines in the system.

Preprints (www.preprints.org) | NOT PEER-REVIEWED | Posted: 6 May 2022 doi:10.20944/preprints202205.0057.v1

$$Line(L)_{Rloss} = R_w - R_p \tag{12}$$

$$Total\ Reactive\ Power\ losses = \sum_{l=1}^{nl} Line(L)_{Rloss} \tag{13}$$

RPI is the reactive power loss index which is expressed as a ratio of RP_{LDG} to RP_L. The process is given by Eq. (14), where RP_{LDG} and RP_L are reactive power losses with and without DG, respectively.

$$RPI = [RP_{LDG} / RP_L] \tag{14}$$

2.2.1.2 Voltage Deviation Index

The voltage deviation index (*VD) is* the third objective that is under consideration for the current problem and is mainly used for monitoring the power system. So, in real-time, voltages across buses deviate from their stability limit and can be set to a safe limit by optimal allocation of DG in a system that eventually helps in the improvement of voltage profile. The *VD* must be small, because of the fact that a higher value corresponds to a more significant deviation from the initial one. The process is given by Eq. (15). n is the total number of buses in the system while V_b is the bus voltage after placement of DG in the system and V_{ini} is the initial voltage and is consider as 1.03 nominal voltage as referred to [16].

$$VD = max_{b=1}^{n} \left(\frac{|V_{ini}| - |V_b|}{|V_{ini}|} \right) \tag{15}$$

2.2.2. Constrains

2.2.2.1. Limitations of DGs Capacity

The active and reactive powers supplied by the DG have a capacity limit (Limit). It is given by Eq. (16). P_{DG} and Q_{DG} *denote* the active and reactive power of the DG, which is measured in kW and kVAR.

$$0 < P_{DG}, Q_{DG} \le Limit \tag{16}$$

2.2.2.2. Power Balance

The power supplied by each DG and Grid must be equal to load and losses [10].

$$\sum P_{DG} + P_{Grid} = \sum P_{load} + P_{loss} \tag{17}$$

$$\sum Q_{DG} + Q_{Grid} = \sum Q_{load} + Q_{loss} \tag{18}$$

P_{DG} and Q_{DG} are active and reactive powers supplied by each DG, respectively, while P_{Grid} and Q_{Grid} are active and reactive power from the grid station. The active and reactive load of the system is denoted by P_{Load} and $Q_{Load,}$ respectively while active and reactive power losses of the system are P_{Loss} and $Q_{Loss,}$ respectively.

3. Optimization Algorithms

The methodology utilizes the BRO, APSO, and GA metaheuristic algorithms for optimum DG allocation described in the following sections.

3.1. Battle Royal Optimization Algorithm

BRO is a metaheuristic algorithm which is basically inspired by the idea of royal battle games such as PUBG and Call of Duty. The algorithm was developed by Taymaz [29] in 2020 and is first time used in this paper for optimal placement of DGs in the system. This algorithm envisages that each player must be randomly placed in the game space encompassing same amount of resources and strength. Wherein, each player has to compete with the other players and game-obstacles as well. Every player in the game tries to move towards a safe

Preprints (www.preprints.org) | NOT PEER-REVIEWED | Posted: 6 May 2022 doi:10.20944/preprints202205.0057.v1

region and kill the opponent player. On the losing end, players' resources or strength might be reduced or they may be eliminated from the game on the account of damage. In the end, the player possessing highest number of kills finally wins the game. The main steps of the BRO algorithm are listed below;

Step I: This step accounts for initialization of algorithm parameters by determining the number of population, iterations and maximum threshold.

Step II: Random population is generated within the problem space.

Step III: Each individual in the game tries to hurt the nearest opponent soldier.

Step IV: The soldier hurt by an opponent loses one point of strength.

Step V: The player, which experiences damage, tries to alter its position. The position within dimension (*dim)* can be achieved by Eq. (19).

$$x_{D,dim} = x_{D,dim} + r(x_{B,dim} - x_{D,dim}) \tag{19}$$

Wherein, $x_{D,dim}$ represents the position of the damaged soldier, while $x_{B,dim}$ represents the position of best soldier found so far. r denotes a random number which is uniformly distributed from the range of 0 to 1.

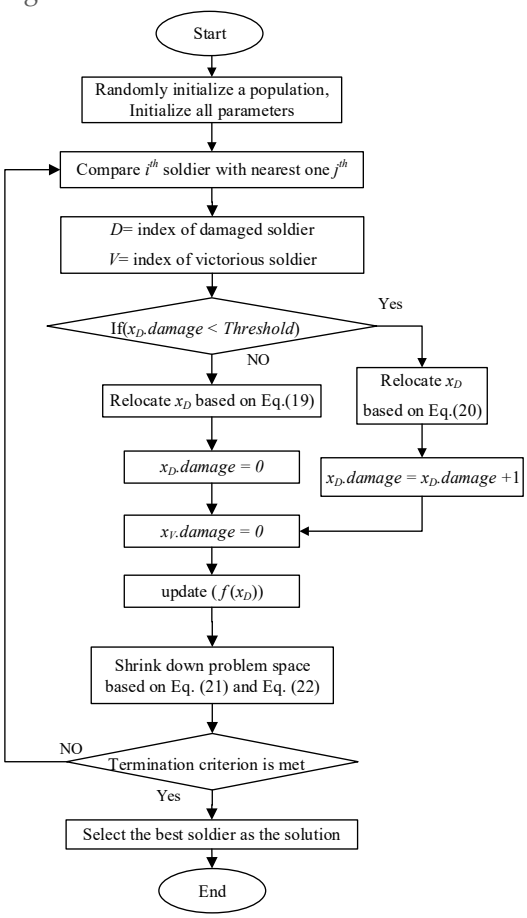

Figure 2. Flow Chart of BRO Algorithm

Step VI: If the soldier's strength reduces up to the extent of predefined threshold due to damage, then this soldier dies. The player will be reallocated within the feasible region with full strength. The process is given by Eq. (20).

$$x_{D,dim} = r(ub_{dim} - lb_{dim}) + lb_{dim} \tag{20}$$

In Eq. (20), ub_{dim} and lb_{dim} are the upper and lower bounds of dimension, whereas r has a random value between 0 and 1.

Step VII: In this step, after each iteration, the search space converges towards the best solution. The process is illustrated by Eq. (21) and Eq. (22). Wherein, *SD corresponds to the*

Preprints (www.preprints.org) | NOT PEER-REVIEWED | Posted: 6 May 2022 doi:10.20944/preprints202205.0057.v1

standard deviation of the population. Moreover, lb_{dim} and ub_{dim} are the upper and lower bound limits of dimension *dim*, respectively.

$$lb_{dim} = x_{B,dim} - SD\left(\overline{x_d}\right) \tag{21}$$

$$ub_{dim} = x_{D,dim} + SD\left(\overline{x_d}\right) \tag{22}$$

Step VIII: In this step after the completion of each iteration, the best solution is selected.

The flow chart of BRO is shown in Figure 2**.** For the sake of DGs' allocation, following alterations are made in the conventional BRO. outlined:

- The population of soldiers is replaced with DGs' locations and sizes.
- The threshold selected in the current paper is 3 and specific value is used to avoid premature convergence and to attain improved results.[29]
- The upper and lower bounds are replaced with the upper and lower limits of DGs' location and size.

The best solution depends on a multi-objective value.

3.2. Accelerated Particle Swarm Optimization Algorithm

APSO is the updated version of PSO and was developed by Yang in 2010 [30]. The study [31] consider APSO for optimal DG allocation. In PSO, both global best and particle best positions are used. The diversity in this algorithm is achieved by using particle's best position while for the sake of expeditious convergence, only global best position (P_g) is used in APSO. The algorithm is discussed and utilized in [32]. The velocity vector at *t+1* iteration is obtained by using Eq. (23).

$$V_j^{t+1} = V_j^t + \alpha\varepsilon + \beta\left(P_g - X_j^t\right) \tag{23}$$

For convergence of algorithm more rapidly, the particle's location is also updated using Eq. (24) where ε is the vector containing random values between 0 and 1.

$$X_j^{t+1} = \left(1-\beta\right)X_j^t + \beta P_g + \alpha\varepsilon \tag{24}$$

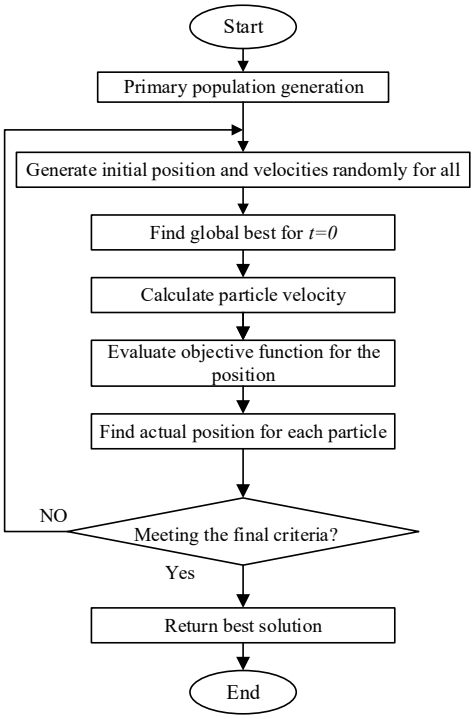

Figure 3. Flow Chart of APSO Algorithm

The particular values of α lie within 0.1 to 0.4 while the value of β is between 0.1 and 0.7. *t* is the index value of each iteration and also used in flow chart. In the current problem, the

Preprints (www.preprints.org) | NOT PEER-REVIEWED | Posted: 6 May 2022 doi:10.20944/preprints202205.0057.v1

value of alpha α is 0.2 while beta β is taken as 0.5 [30]. The position in the APSO algorithm is replaced with DG size and location. The flow chart of the APSO algorithm is shown in Figure 3 [33]. APSO algorithm comprised of following stages that are illustrated below. [32].

Step I: The first step accounts for the initialization of basic parameters of the algorithm such as population, velocity and number of iterations.

Step II: Similarly second step accounts for, evaluation of objective function value at each particle's location.

Step III: In this step calculation of global best position will be carried out.

Step IV: After locating global best position the algorithm will update the swarm velocity and position using Eq. 13 and Eq.14.

Step V: At the end, repetition of step 2 is done until the specific criteria are satisfied.

3.3. Genetic Algorithm

Genetic algorithm (GA) is an evolutionary optimization technique based on genetics phenomena and Natural Selection. Hence, the best candidate is always chosen by the Natural Selection process, which is dominant over the weaker ones [34]. The study [35] also implemented GA for optimal DG allocation. The flow chart of GA is illustrated in Figure 4 [36].

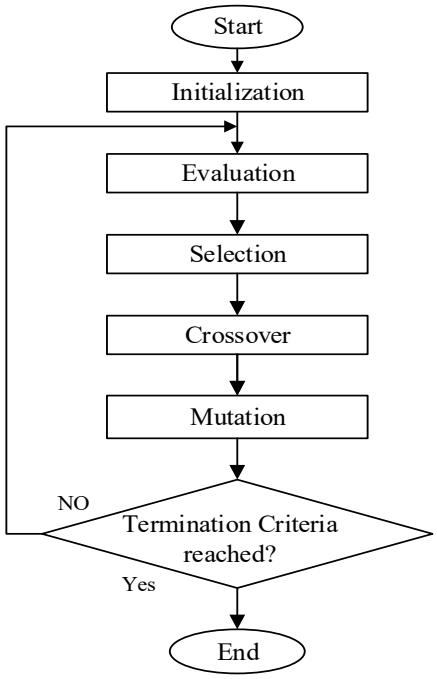

Figure 4: Flow Chart of GA

This process involve Selection, Crossover and Mutation, while basic steps of methods are discussed below.

Step I: First of all, the initial chromosome population is generated, while in the current case, DGs sizes and locations are reciprocated as chromosomes.

Step II: Second step accounts for evaluation of the fitness value of each chromosome in the population.

Step III: New population is generated using biological evaluation, which is selection, crossover, mutation and at the last acceptance.

Step IV: In last step, check the results if achieved up to the desired range; otherwise, repeat the process from fitness calculation.

Preprints (www.preprints.org) | NOT PEER-REVIEWED | Posted: 6 May 2022 doi:10.20944/preprints202205.0057.v1

4. Mathematical Modelling of Optimization Problem

This section envisions min-max regret criteria for the optimal allocation of DG all, modelling of the said optimization problem and the test systems employed to cope up the optimization problem.

4.1. Min-max Regret Criteria

The min-max regret criteria provide a robust solution for various scenarios while minimizing the worst-case regret [37]. It means that the min-max regret criteria calculates the best possible solution for all possible scenarios. Aforementioned solution then minimizes the maximum divergence between the best possible solution and the optimal solution of each corresponding scenario. The said technique has been applied and implemented in [37,38]. Wherein, *S* is considered as a finite set of scenarios (*s1,s2,s3,….sn*) and, each scenario *s* is the subset of *S* i-e (s∈S). Herein, set of solutions is represented by vector *X* (*x1,x2,x3,…..,xn*). *f(x,s)* is represents the value of solution x∈X at scenario s∈S and x_s^* is the optimal solution at scenario s∈S and $f_s^*= f(x_s^*,s)$ is the corresponding optimal value. In first step, regret value *R(x,s)* of each solution *x* under scenario *s* is obtained, which is represented by the following equation.

$$R(x,s) = f(x,s) - f_S^* \tag{25}$$

The maximum regret value of solution x∈X is denoted by $R_{max}(x)$ which can be further expressed as $R_{max}(x)= maxR_{max}(x,s)$. In second step the maximum regret value of each solution is obtained. In the end, the solution which possess the minimum value among the corresponding maximum regret values is considered the minimum solution of all the solution x∈X and is defined by the following equation.

$$\min R_{\max}(x) = \min \max_s \left(f(x,s) - f_S^* \right) \tag{26}$$

4.1.1. Handling DG Allocation Through Min-max Regret Criteria

The min-max regret criteria is implemented for the Day-ahead bidding strategies in [38], which inspired to implement for current DG allocation problem incorporating multiple scenarios. The min-max regret criteria for DG allocation (at various scenarios) need several replacements in the corresponding equation of min-max regret criteria. DGs' allocation (sizes and locations) is considered as solution x. First step corresponds to the selection of best allocations of DGs that are obtained at each scenario that are further considered as solutions (*x1, x2, x3,…xn*) and considered in vector *X*. The value of solution is *f(x,s)* and regret value *R(x,s)* are replaced with *MO* and fitness value *F* in the current method respectively. *OMO* refers to the optimal multi-objective index value which is considered as optimal MO value. OMO_s is defined as f_s^* in Eq. (25) which is the optimal value of *x* at particular scenario *s*. *MO* is obtained by each solution *x* at particular scenario *s*. Total 24 scenarios are taken and considered as a set *S (S=(s1,s2,s3,…..s24))* while each scenario signifies the specific hour of the day. In second step, *F* is obtained for each solution *x* as a regret value for the particular scenario. The general equation mentioned earlier Eq. (25) for the calculation of the regret value of solution *x* is modified according to current method and illustrated below.

$$F_{(x,s)} = MO - OMO_s \tag{27}$$

In third step, the maximum regret value of each solution *x* is obtained by Eq. (28).

$$\max F_{(x)} = \sum_{s=1}^{s=24} F_{(x,s)} \tag{28}$$

$$MF = \max F_{(x)} \tag{29}$$

Maximum regret value is defined in terms of $maxF_{(x)}$, which is the arithmetic sum of all *F* values of each solution x. Eq. (26) is modified in accordance to the current problem of DGs allocation that is represented by Eq. (30) is mentioned hereunder;

Preprints (www.preprints.org) | NOT PEER-REVIEWED | Posted: 6 May 2022 doi:10.20944/preprints202205.0057.v1

$$\min MF_{(x)} = \min \max MF_{(X)} \tag{30}$$

Wherein, the solution x, which has a minimum value *maxf(x)* is considered as the final solution. From fourth to tenth step modelling of the optimization problem has been carried out that includes the min-max criteria.

4.2. Modelling Of The Optimization Problem

The main focus of current paper envisages on the improvement of the power system while minimizing power system losses (active and reactive) and improving bus voltage profiles. The study is carried out under a 24h load horizon and renewable generation. This method involves the concept of min-max regret to obtain a robust solution that incorporates optimal allocation of DGs in the system. A total of 24 different scenarios are considered, and each of them has a unique load and renewable generation profile.

First of all, the NRLF analysis is carried out for each scenario in order to obtain optimum parameters of DGs, which are to be introduced in the system. Consideration of DGs are realized on the basis of minimum values of MO while using GA, APSO and BRO respectively. Furthermore, the obtained DGs are placed in the test system one by one to in order to calculate the fitness values for each DG in a considered scenario. Afterwards, the maximum fitness value of the DG is obtained by summation of all fitness values of the DG across all scenarios respectively. Hence, the DG devouring the least maximum fitness value is considered as the desired optimal allocation of the DG for 24 hours. Aforementioned approach corresponds to the novelty as compared to the concurrent methods, as it studies the active and reactive power loss minimization and enhancement in bus voltage profiles for 24 hours with a time step of one hour. The flow chart of the earlier discussed methodology is shown in Figure 5. Steps for achieving the desired objectives are mentioned hereunder;

Step I: Initialize basic parameters of BRO, GA and APSO algorithms and set the population size and number of iterations.

Step II: Perform newton-raphson load flow (NRLF) without integrating DG (/s) in the system and calculate APL and RPL for each scenario / hour. Renewable DGs produce different power for each particular scenario on the account of fluctuating nature of solar and wind. Moreover, the load is also fluctuating in each scenario which is that depends upon the demand side.

Step III: Find DG (/s) with the optimal allocation (i.e. sizes and locations) for each scenario based on minimum *MO* values calculated through BRO, GA and APSO algorithms.

$$DGC = \left[dg1 \;\; dg2 \;\; dg3 \right] \tag{31}$$

$$MO_{S=1,2,3,\ldots,24}$$

In Eq. (31), *DGC* represents the combination of DGs that would be placed in the test system, *dg* represents the optimal allocation of DG, whereas the coefficient of *dg* denotes the exact number of DGs allocated in the test system. The optimal allocation of DG means the optimal size and location of DG. *S* represents the scenario.

Step IV: Sort *MO* values in ascending order that are obtained for each scenario. Onward, select ten best *DGC* corresponding to ten minimum *MO* values of the particular scenario. As a whole 24 scenarios are formed for a day and so each specific scenario is studied for each hour. Therefore *S* reaches up to 24.

$$MO_{S=1,2,..,24} = \left[MO1\, MO2\, MO3 \ldots\ldots MO10 \right] \tag{31}$$

$$DGS_{S=1,2,..24} = \left[DGC1\, DGC2\, DGC3 \ldots DGC10 \right] \tag{32}$$

Wherein Eq. (32), MO_S is the set of minimum *MO* values obtained for scenario *S*, *MO1* to *MO10* are sorted minimum *MO* values for scenario S. In Eq. (33), DGS_S is the set of DGCs (i.e. DGC1 to DGC10) selected corresponding to minimum *MO* values obtained for the same scenario *S*. Ten *DGCs* are obtained per scenario resulting a total of 240 *DGCs* for 24 scenarios.

Preprints (www.preprints.org) | NOT PEER-REVIEWED | Posted: 6 May 2022 doi:10.20944/preprints202205.0057.v1

Step V: Place *DGC* in the system one by one and calculate AP_{LDG}, RP_{LDG} and V_b for each scenario.

Step VI: Calculate *MO* for each *DGC* by using Eq. (8). In each scenario, it is carried out while considering the parameters AP_L, RP_L, AP_{LDG}, RP_{LDG} and V_b that were calculated during Step II and Step V.

$$MO_{DGC1} = [MO_{S1}, MO_{S2}, ..., MO_{S24}] \quad (34)$$
$$MO_{DGC2} = [MO_{S1}, MO_{S2}, ..., MO_{S24}]$$
$$\ldots\ldots\ldots$$
$$MO_{DGC240} = [MO_{S1}, MO_{S2}, ..., MO_{S24}]$$

Herein Eq. (34), MO_{DGC1} to MO_{DGC240} are the set of *MO* values, calculated by placing the *DGC1* to *DGC240* respectively for all 24 scenarios. Similarly, MO_{S1} to MO_{S24} are *MO* values that are calculated for specific *DGC* from scenario *S1* to scenario *S24*.

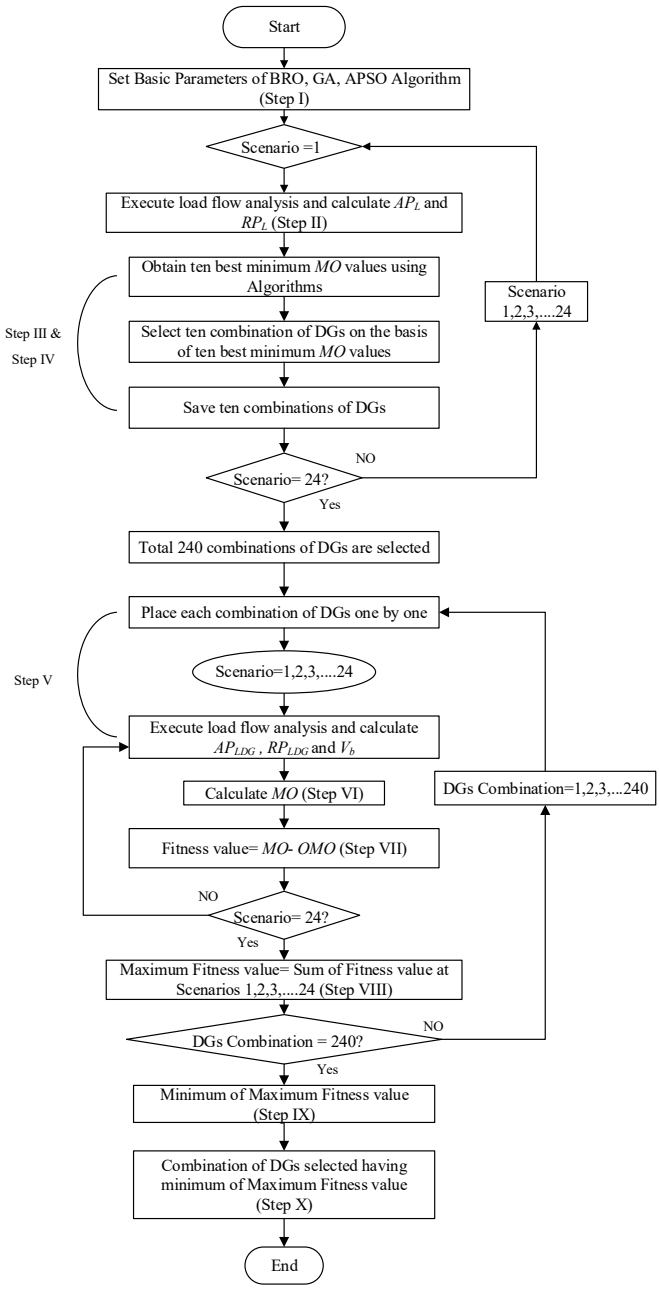

Figure 5. Methodology

Preprints (www.preprints.org) | NOT PEER-REVIEWED | Posted: 6 May 2022 doi:10.20944/preprints202205.0057.v1

Step VII: Compute fitness value *F* for particular DGC under scenarios S1 to S24 using Eq. (36).

$$OMO = \left[OMO_{S1}, OMO_{S2}, \ldots\ldots, OMO_{S240}\right] \tag{35}$$

$$F_{DGC1,S1} = \left[MO_{S1} - OMO_{S1}\right] \tag{36}$$

$$F_{DGC1,S2} = \left[MO_{S2} - OMO_{S2}\right]$$

$$\ldots\ldots\ldots$$

$$F_{DGC1,S24} = \left[MO_{S24} - OMO_{S24}\right]$$

In Eq. (35), *OMO* is the set of optimal *MO* values obtained for all scenarios, whereas OMO_{s1} *to* OMO_{s24} are optimal values for scenarios *S1* to *S24*. Although, the optimal *MO* value means the maximum achievable minimum *MO* value.

Step VIII: Calculate maximum fitness value MF by calculating arithmetic sum of all fitness values of the particular DGC using Eq. (37).

$$MF_{DGC1} = \sum_{S=1}^{S=24}\left(F_{DGC1,S1,}F_{DGC1,S2,},\ldots,F_{DGC1,S24}\right) \tag{37}$$

$$MF_{DGC2} = \sum_{S=1}^{S=24}\left(F_{DGC2,S1,}F_{DGC2,S2,},\ldots,F_{DGC2,S24}\right)$$

$$\ldots\ldots\ldots$$

$$MF_{DGC240} = \sum_{S=1}^{S=24}\left(F_{DGC240,S1,}F_{DGC240,S2,},\ldots.,F_{DGC240,S24}\right)$$

Step IX: Sort MF of all DGCs and find the minimum of maximum fitness among all DGCs by using equation mentioned hereunder;

$$\min MF = min\left[MF_{DGc1}, MF_{DGc2}, \ldots., MF_{DGc240}\right] \tag{38}$$

Step X: The combination of DGs (i.e. *DGC*) with the least value of *MF* is considered the desired solution for all scenarios.

4.3. Test System

This paper considered CIGRE MV benchmark model as a test system for implementing the optimization problem discussed in the above section.

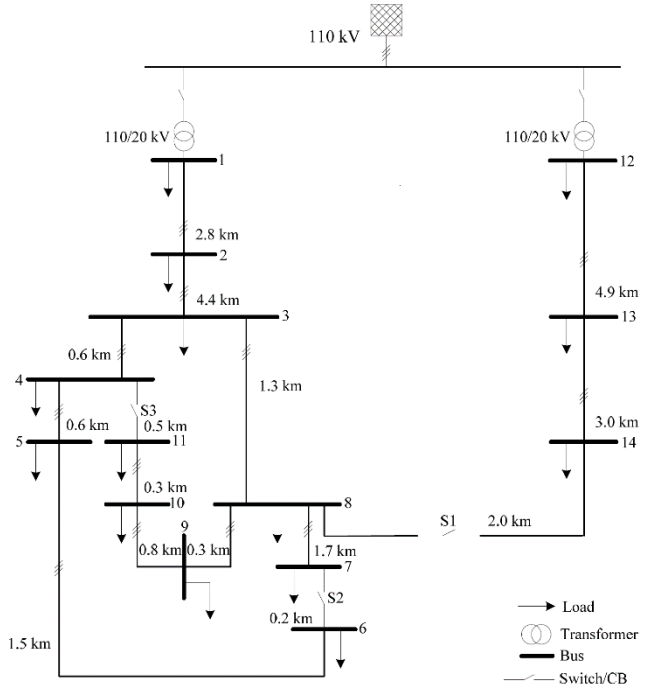

Figure 6. CIGRE MV Benchmark Model

Preprints (www.preprints.org) | NOT PEER-REVIEWED | Posted: 6 May 2022 doi:10.20944/preprints202205.0057.v1

4.3.1. CIGRE MV Benchmark Model

The model consists of 14 buses and 15 branches, as shown in Figure 6. Different types of DGs are connected to altered buses in the test system [39]. Almost every DG type has stable output power, but two of them have variations in output power on the account of fluctuation in the resources at different time of the corresponding day. Aforementioned DGs encompass solar and wind utility resources. The model also includes a battery but is neglected in this study because of its charging and discharging behavior after a specific period.

4.3.2. Simulation Setup

The optimal allocation of DGs for 24-hour load horizon is already discussed in the methodology section which is executed by various algorithms. Aforementioned simulations are carried on MATLAB. The parameters of each algorithm are listed in Table 2.

Table 2. Parameters of Algorithms

Parameters	BRO	APSO	GA
No. of Iterations	100	100	100
Population Size	100	100	100
Size Range of DGs (kW and kVAR)	10 ~ 500	10 ~ 500	10 ~ 500

4.3.3. Input Data Configuration

The 24-hour load data is utilized for the CIGRE model with a time step of one hour [40]. The residential and commercial loads are connected to different buses with different power factors. The net active and reactive power loads connected to the European version of the CIGRE model are calculated on an hourly basis. The active and reactive power load values for each specific hour are outlined in Appendix A (Table A1 and Table A2). In Table A1 and Table A2, the left-most column "Time (Hrs)" represents the time of the day in hours. In the CIGRE model, four different ratings, i.e., 40kW, 30kW, 20kW, and 10kW of solar DGs, are already installed, while the output power curve of each type of DG rating is shown in Figure 5(a). Each curve corresponds to the product of the power per unit curve of PV [41] and the rating of the solar DG. The wind DG used in the CIGRE model has a rating of 1500 kW, while power extracted at each scenario from the DG is shown in Figure 5(b). The wind power curve is the product of its rating and wind DG per unit curve [33]. Scenario represents the specific hour of the day.

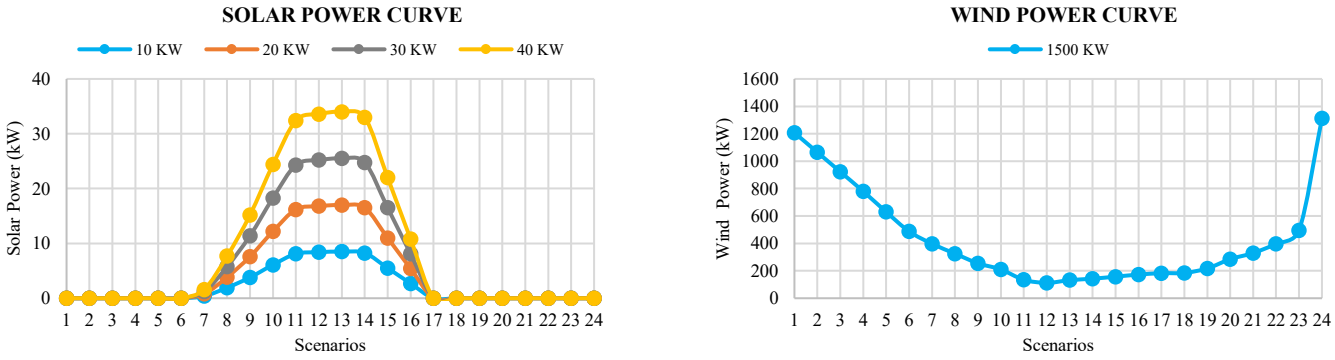

(a) (b)

Figure 5. Power Curve (a) Solar (b) Wind

5. Results

This section exhibits the effectiveness of the proposed methodology and algorithms on CIGRE's MV Benchmark model. It permits computing the voltages across all buses and

Preprints (www.preprints.org) | NOT PEER-REVIEWED | Posted: 6 May 2022 doi:10.20944/preprints202205.0057.v1

active and reactive power losses for a system overall and on lines. The study has been conducted by the placement of three DGs in the test system. These DGs have the same active and reactive power that is expressed in kW and kVAR. The minimum capacity limit is 10k, whereas the maximum limit accounts for 500k. In the said model, twenty-four different scenarios are considered. Each scenario corresponds to a single hour of the respective day and has a unique load and generation profile. In each scenario, the load and power of solar and wind DGs fluctuate. The active and reactive power loss minimization procedure is carried out according to the methodology mentioned earlier. Three DGs are incurred in the CIGRE model by optimizing system constraints (i.e., optimal size and location). Each DG among them has been used for the consideration executing mentioned algorithm for all scenarios. At the initial stage, ten best optimal allocations of DGs are obtained for each scenario, and 240 optimal allocations are considered for 24 scenarios. Among these 240 solutions, the best one is selected using the min-max regret criteria. The best optimal allocation of DGs at each particular scenario is represented in Table 3. The robust optimal locations and sizes of DGs for all 24 scenarios are obtained through min-max criteria and represented in Table 4. However, the locations and sizes obtained as modes and an average of 20 results respectively as the whole methodology is carried out 20 times. Hence, all other results are deduced by extracting their average values.

Table 3. Optimal DGs' Allocations at each scenario

Scenarios	APSO		GA		BRO	
	DG Locations	DG Sizes	DG Locations	DG Sizes	DG Locations	DG Sizes
1	1,2,12	171.30,10,43.87	12,1,2	51.35,214.26,14.73	2,1,12	15.51,162.58,40.43
2	1,12,2	166.89,24.50,10	12,1,2	24.37,205.93,57.49	2,1,12	14.78,168.37,25.66
3	2,1,12	10,158.81,19.60	12,1,2	65.80,413.49,50.08	2,1,12	18.66,174.74,23.16
4	13,1,12	10,166.26,24.47	2,12,1	10.14,28.47,146.75	1,2,8	135.25,43.98,11.57
5	1,12,8	194.65,41.99,10	2,1,12	32.49,173.65,39.49	12,1,2	40.54,169.10,21.74
6	12,1,2	81.44,172.96,10	12,1,13	61.33,198.32,26.40	12,8,1	84.15,12.57,240.66
7	1,6,12	200.19,10,116.28	1,12,13	235.07,99.55,33.70	1,12,13	216.04,105.89,24.47
8	1,2,12	178.15,10,129.19	12,2,1	127.44,55.41,201.71	13,1,12	16.55,179.16,114.01
9	1,2,12	177.58,10,127.21	2,1,12	42.21,238.37,136.20	2,1,12	51.20,202.74,127.79
10	12,1,8	131.33,196.0,10	12,13,1	126.07,13.87,205.31	12,2,1	136.29,31.52,207.41
11	12,6,1	111.92,10,199.07	13,12,1	21.92,97.80,194.21	2,1,12	21.21,203.31,116.99
12	12,13,1	127.28,10,185.68	2,12,1	53.44,131.12,203.13	1,12,2	227.45,136.17,77.57
13	1,2,12	178.40,10,124.37	12,1,2	126.32,202.01,21.50	14,1,12	11.28,187.81,113.93
14	13,1,12	10,182.84,106.16	12,2,1	109.70,35.14,186.68	1,8,12	186.22,13.79,104.92
15	2,1,12	10,174.06,103.36	2,12,1	72.13,98.57,204.19	1,2,12	208.96,96.62,96.12
16	2,1,12	10,172.15,95.42	12,2,1	84.97,135.51,219.17	12,1,2	89.80,206.86,60.59
17	1,2,12	177.77,109.28,10	1,2,12	190.36,33.58,107.72	1,12,2	184.21,99.20,90.54
18	12,1,2	127.56,18.48,10	13,12,1	29.45,107.84,214.17	13,1,12	29.10,249.02,115.30
19	12,8,1	139.92,10,201.15	1,13,12	243.72,55.93,105.24	12,13,1	134.70,15.65,208.25
20	8,12,1	10,124.32,201.26	2,1,12	10,183.09,126.88	1,2,12	190.74,49.36,122.56
21	8,12,1	10,10.86,198.24	2,1,12	10.02,176.03,104.47	2,12,1	44.88,98.21,152.83
22	2,12,1	10,87.56,177.39	1,2,12	173.30,10,87.15	8,1,12	11.12,207.20,86.28
23	8,12,1	10,59.63,187.21	2,1,12	36.33,213.13,66.79	8,12,1	11.64,57.52,180.04
24	8,12,1	10,35.87,187.81	12,1,2	23.07,89.04,19.91	2,1,12	54.13,200.46,35.66

Preprints (www.preprints.org) | NOT PEER-REVIEWED | Posted: 6 May 2022 doi:10.20944/preprints202205.0057.v1

Table 4. Optimal DGs' Sizes and Locations for all scenarios

Algorithms	DG 1 Location	DG 2 Location	DG 3 Location	DG 1 Size (*1000)	DG 2 Size (*1000)	DG 3 Size (*1000)
GA	1	12	2	181.119	62.568	10.504
APSO	1	12	2	208.643	70.117	33.410
BRO	1	12	2	200.221	69.168	29.152

Table 5. Optimal MO Values

Scenarios	BRO	GA	APSO	Scenarios	BRO	GA	APSO
1	0.5027	0.5143	0.5027	13	0.0973	0.1006	0.1070
2	0.5643	0.5643	0.5642	14	0.1207	0.1245	0.1207
3	0.6560	0.5580	0.5580	15	0.1433	0.1474	0.1567
4	0.5642	0.5642	0.5642	16	0.1683	0.1682	0.6334
5	0.4984	0.4869	0.7834	17	0.1416	0.1332	0.1292
6	0.2326	0.2326	0.2537	18	0.0934	0.0933	0.1027
7	0.1118	0.1118	0.1083	19	0.0734	0.0734	0.0762
8	0.0893	0.0924	0.0924	20	0.0953	0.0953	0.1048
9	0.1015	0.0922	0.0954	21	0.1457	0.1414	0.1456
10	0.0822	0.0822	0.1991	22	0.2060	0.2116	0.2116
11	0.1207	0.1170	0.1170	23	0.3659	0.3570	0.3570
12	0.0920	0.0834	0.0920	24	0.5788	0.5318	0.5318

Table 6. Summary of Results

Algorithm	Before DG	GA	APSO	Proposed BRO
Maximum Fitness	---	6.39	6.69	6.48
V min (pu)	0.4622	0.7326	0.7056	0.7261
V max (pu)	1.0958	1.2269	1.2159	1.2250
P loss (%) Red	0	55.88	53.03	55.69
Q loss (%) Red	0	47.77	46.23	48.47
Min Line Losses (P,Q) (kW,kVAR)	0.346432, 0.498524	1.392466, 1.992093	1.45, 2.074574	1.384796, 1.98112
Max Line Losses (P,Q) (kW,kVAR)	14569.43, 16907.7	6619.197, 9493.322	7199.756, 10325.97	6465.435, 9272.794
Average Active Power loss (All Scenarios)	26617.93	11743.23	12502.73	11794.14
Average Reactive Power loss (All Scenarios)	26805.49	13999.75	14412.65	13813.91
Active Energy loss (All Scenarios) (kWh)	638830.3	281838	300065.4	283059.7
Reactive Energy Losses (All Scenarios) (kVARh)	643331.89	335994.1	345903.6	331534.010

Preprints (www.preprints.org) | NOT PEER-REVIEWED | Posted: 6 May 2022 doi:10.20944/preprints202205.0057.v1

Findings achieved through simulations are summarized in Table 6. DGs' active and reactive powers are the same and are expressed in kW and kVAR, respectively. The optimal MO value for each scenario is calculated at 2000 iterations with 100 population size using all algorithms and values are listed in Table 5.

5.1. MO and Fitness Values

GA, APSO, and BRO are used to find optimal locations and sizes of DGs for the sake of active and reactive power loss minimization and bus voltage improvement. It has been performed by searching out the minimum value of MO for each scenario. The minimum MO values obtained by each algorithm for all scenarios are shown in Figure 7, whereas the MO convergence curve of APSO, GA, and BRO algorithms for a single scenario is shown in Figure 6. The mentioned results depict that APSO has better performance in terms of MO. Furthermore, these MO values are used to calculate the fitness values, for each considered DG, during each scenario. In the next step, the maximum fitness value of all DGs is calculated. These values resulted in 6.39, 6.69, and 6.48 for the APSO, GA, and BRO, respectively. The aforesaid results are mentioned in Table 6.

5.2. Active Power Losses

The active power loss curves for all scenarios using various algorithms are shown in Figure 8. Herein, the orange curve shows the losses before the placement of DGs. A summary of these results is also presented in Table 6. The active power loss curves of branch 1 to branch 15, for all scenarios, are shown in Figure 9, whereas the average active power losses of the branches are represented in Table 7.

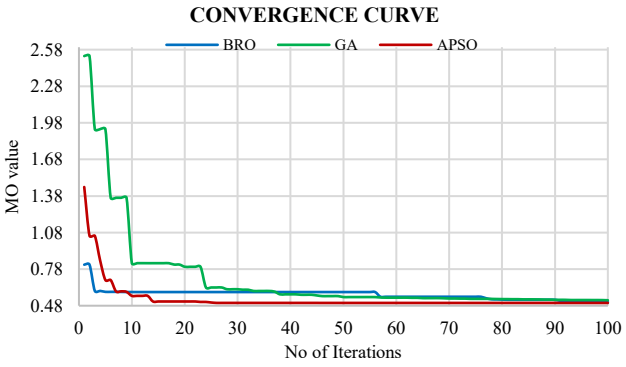

Figure 6. Convergence Curve

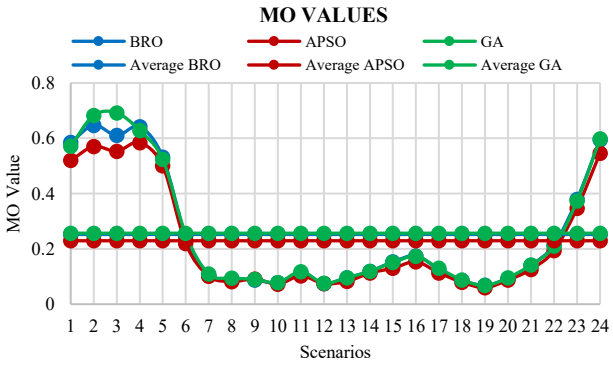

Figure 7. MO Values

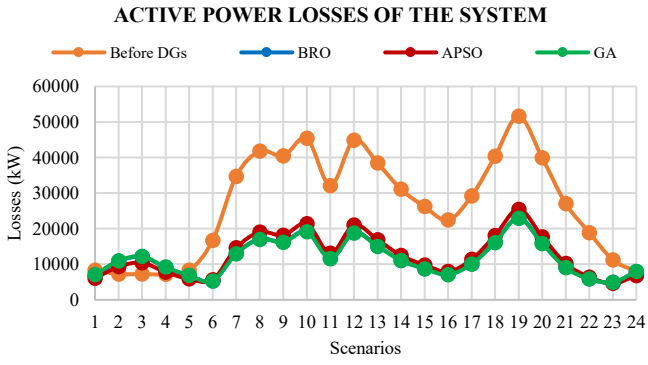

Figure 8. Active Power Losses

Preprints (www.preprints.org) | NOT PEER-REVIEWED | Posted: 6 May 2022 doi:10.20944/preprints202205.0057.v1

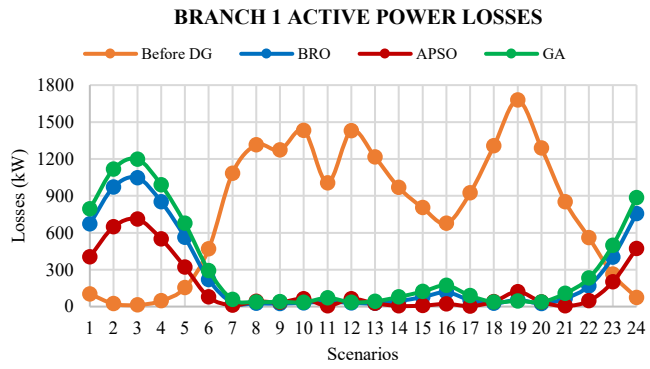

(a)

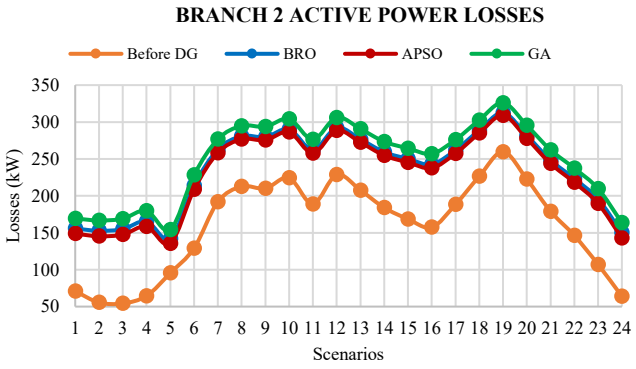

(b)

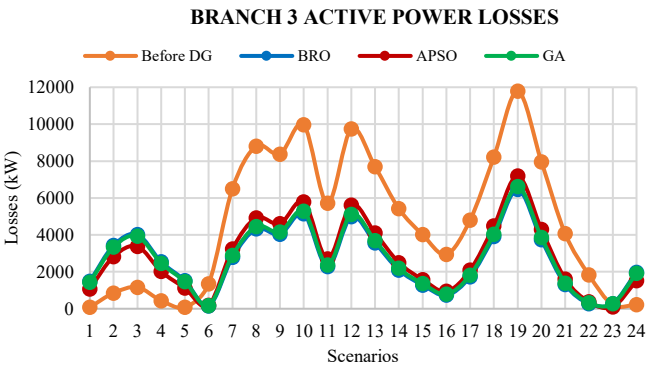

(c)

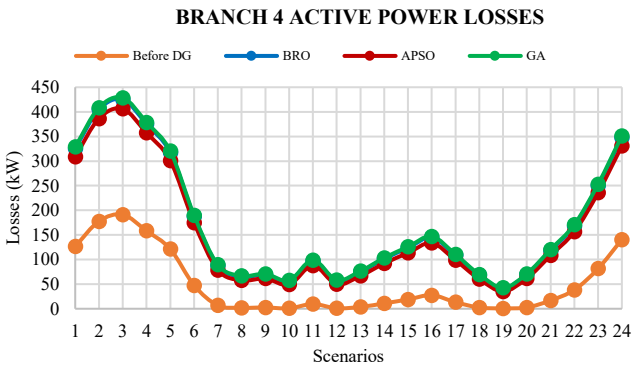

(d)

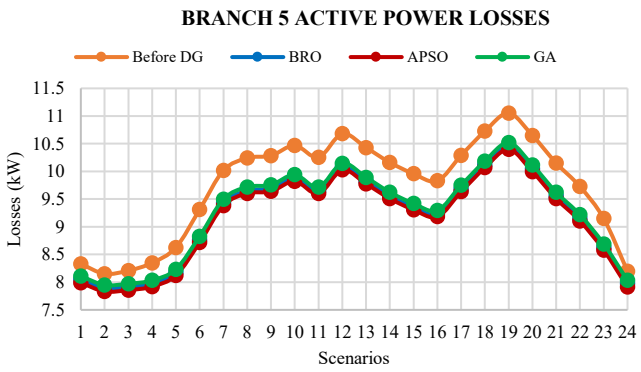

(e)

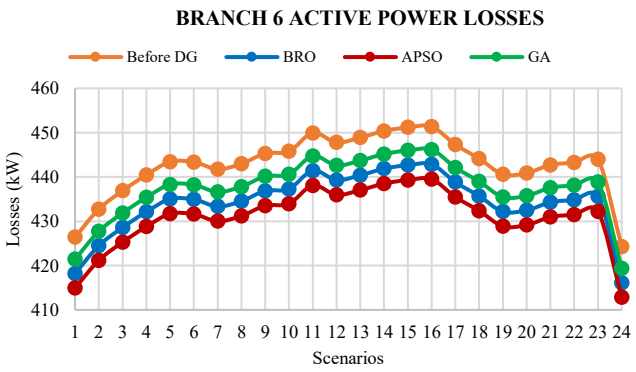

(f)

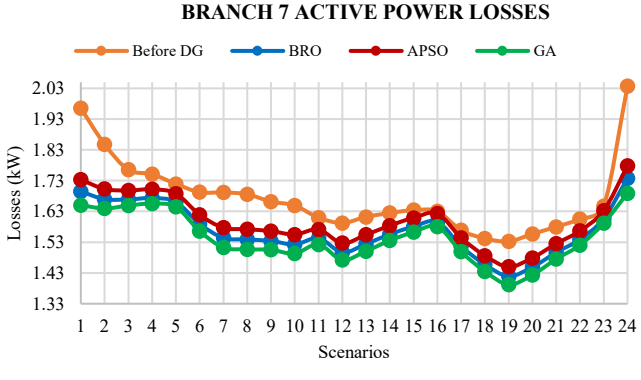

(g)

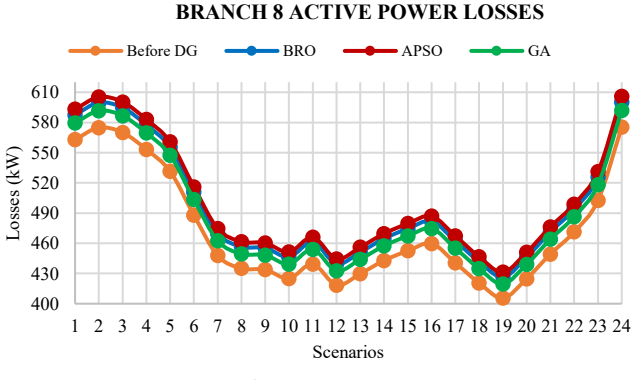

(h)

Preprints (www.preprints.org) | NOT PEER-REVIEWED | Posted: 6 May 2022 doi:10.20944/preprints202205.0057.v1

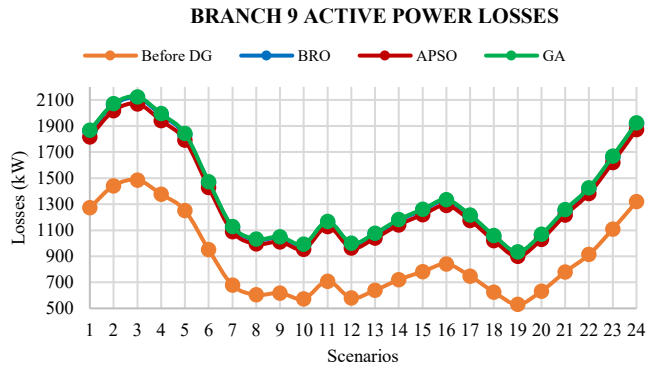

(i)

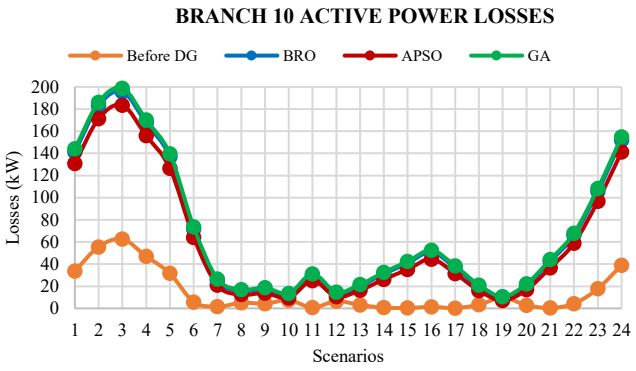

(j)

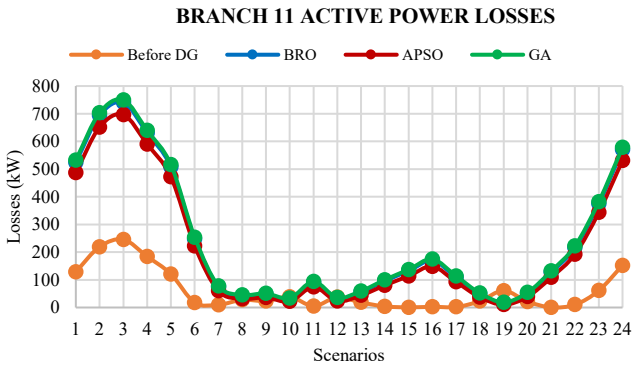

(k)

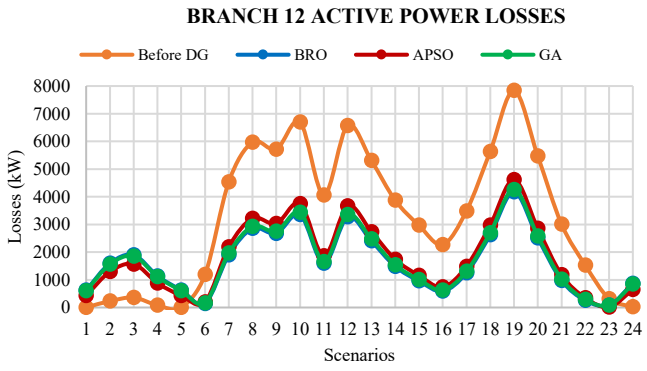

(l)

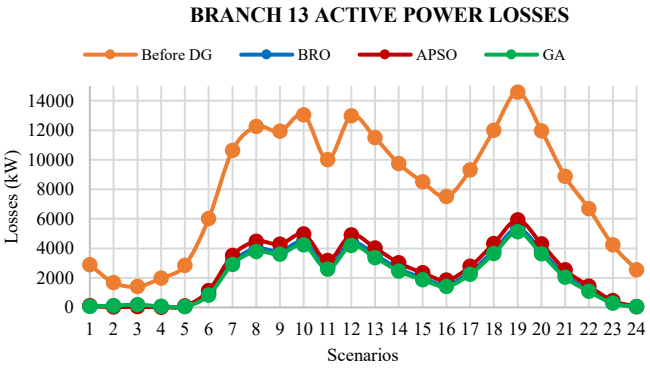

(m)

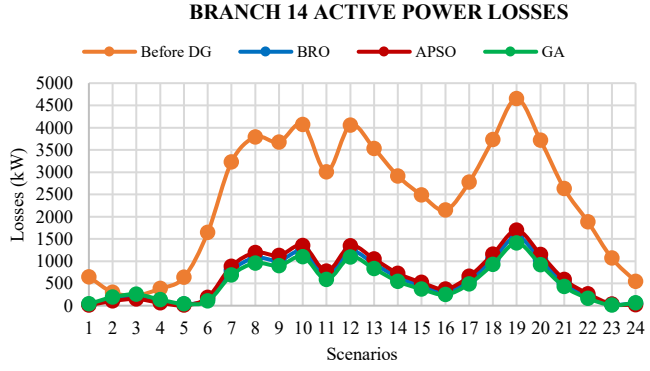

(n)

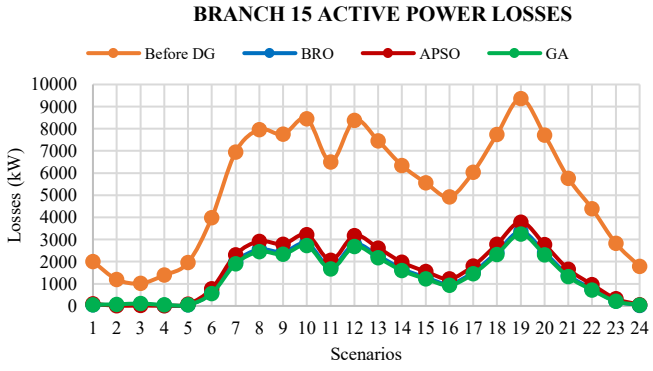

(o)

Figure 9. Active Power Losses of (a) Branch1, (b) Branch2, (c) Branch3, (d) Branch4, (e) Branch5, (f) Branch6, (g) Branch7, (h)Branch8, (i) Branch9, (j) Branch10, (k) Branch11 ,(l) Branch12, (m) Branch13, (n) Branch14, (0) Branch15

Preprints (www.preprints.org) | NOT PEER-REVIEWED | Posted: 6 May 2022 doi:10.20944/preprints202205.0057.v1

5.3. Reactive Power Losses

The reactive power loss curves for each scenario of the studied case are illustrated in Figure 10. A summary of these results is also presented in Table 6. The reactive power loss curves of branch 1 to branch 15, for all scenarios, are shown in Figure 11, whereas average reactive power losses of branches are presented in Table 8.

Table 7. Average Active Power Losses along Branches (kW)

Algorithms	Branch 1	Branch 2	Branch 3	Branch 4	Branch 5	Branch 6	Branch 7	Branch 8	Branch 9	Branch 10	Branch 11	Branch 12	Branch 13	Branch 14	Branch 15
Before DG	789.4	159.9	4678.5	50.1	9.7	442.7	1.7	473.2	882.7	14.4	59.0	3214.7	8124.1	2405.8	5312.2
GA	320.1	249.1	2724.1	172.4	9.3	437.6	1.5	488.2	1381.5	68.8	239.8	1697.0	2074.6	535.3	1343.9
APSO	163.4	230.0	2845.2	158.8	9.1	431.0	1.6	500.7	1337.9	60.5	212.8	1792.6	2489.7	642.7	1626.6
Proposed BRO	263.2	235.1	2671.2	170.2	9.2	434.3	1.5	495.6	1374.3	67.0	234.5	1661.6	2194.6	584.0	1398.0

Table 8. Average Reactive Power Losses of Branches (kVAR)

Algorithms	Branch 1	Branch 2	Branch 3	Branch 4	Branch 5	Branch 6	Branch 7	Branch 8	Branch 9	Branch 10	Branch 11	Branch 12	Branch 13	Branch 14	Branch 15
Before DG	1129.3	228.3	6709.9	71.6	13.9	634.6	2.4	674.2	1268.8	20.7	85.1	4595.2	5829.0	1730.1	3812.3
GA	458.0	355.6	3906.9	246.3	13.2	627.2	2.2	695.8	1985.9	99.0	345.9	2425.8	1488.5	385.0	964.4
APSO	233.7	328.4	4080.6	226.9	13.1	617.8	2.3	713.6	1923.2	87.0	307.1	2562.4	1786.4	462.2	1167.3
Proposed BRO	376.5	335.7	3831.0	243.1	13.1	622.5	2.2	706.3	1975.5	96.4	338.2	2375.1	1574.6	420.0	1003.3

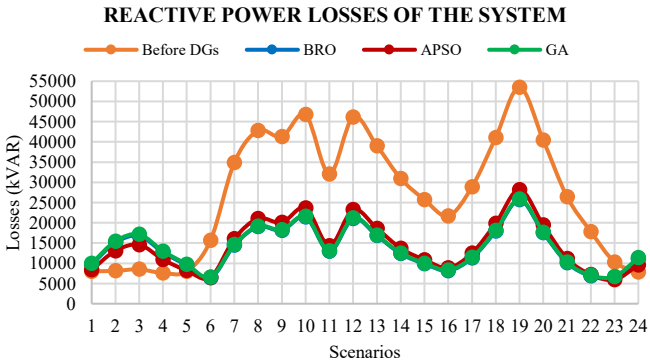

Figure 10. Reactive Power Losses

Preprints (www.preprints.org) | NOT PEER-REVIEWED | Posted: 6 May 2022 doi:10.20944/preprints202205.0057.v1

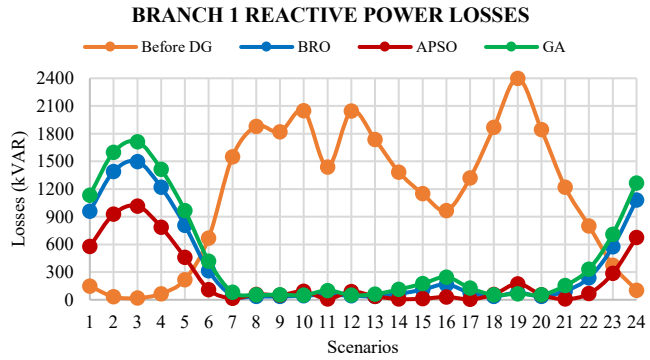

(a)

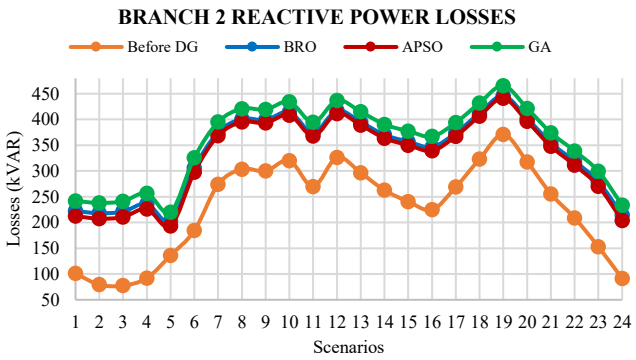

(b)

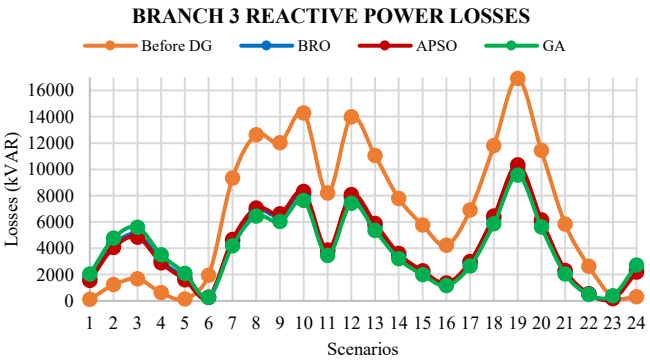

(c)

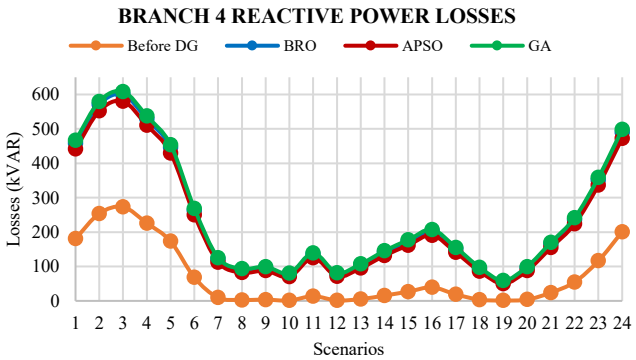

(d)

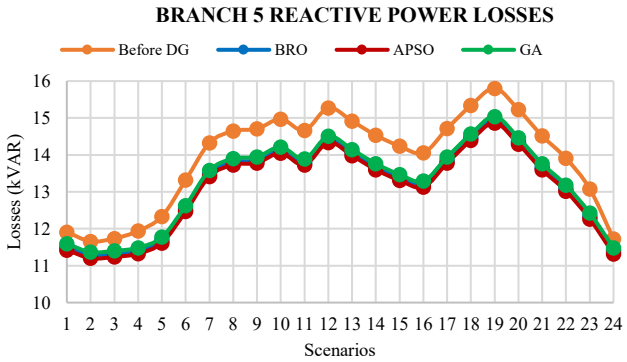

(e)

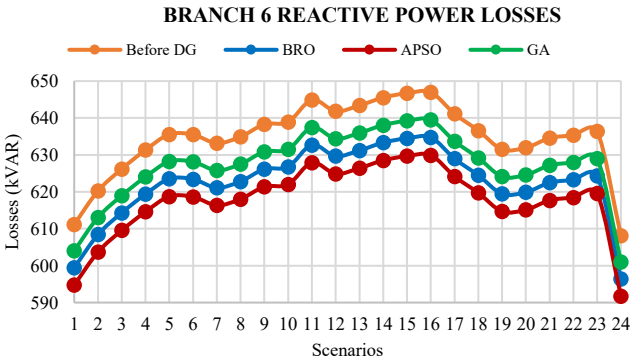

(f)

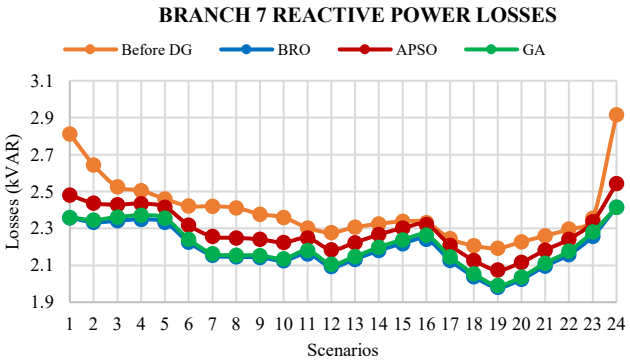

(g)

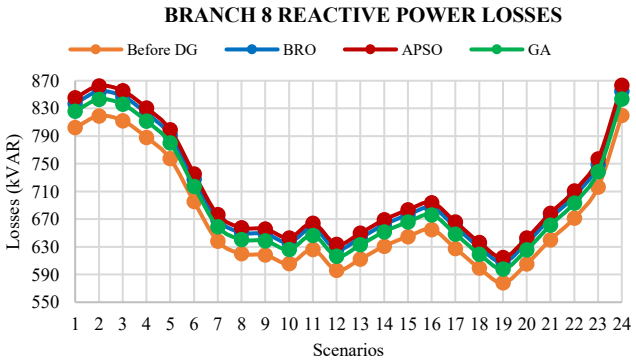

(h)

Preprints (www.preprints.org) | NOT PEER-REVIEWED | Posted: 6 May 2022 doi:10.20944/preprints202205.0057.v1

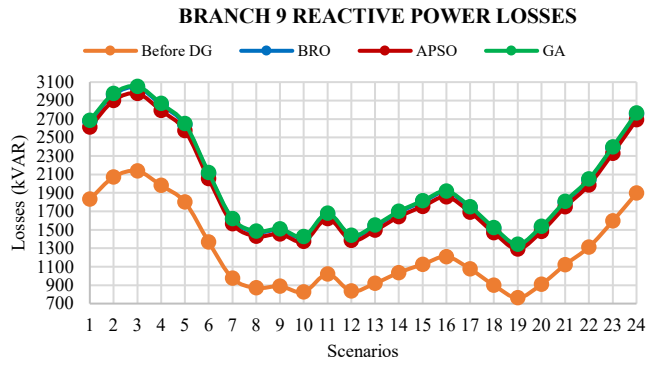

(i)

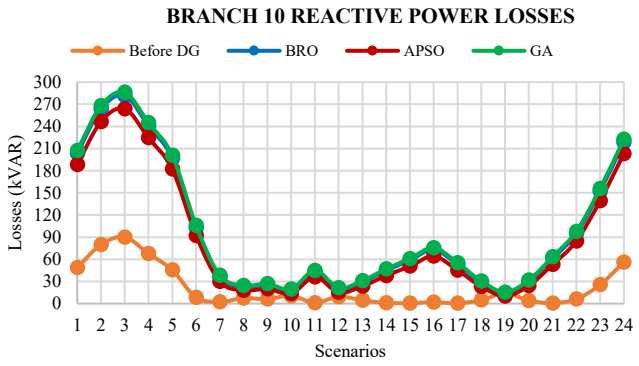

(j)

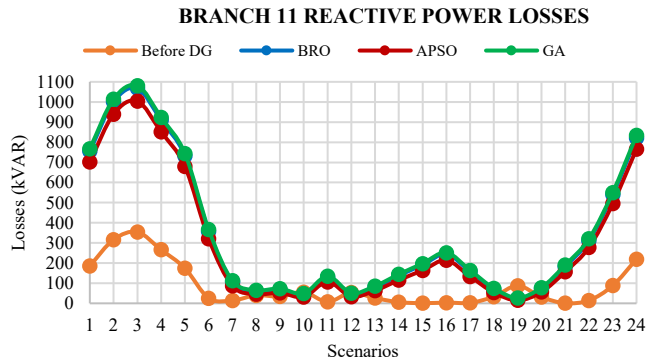

(k)

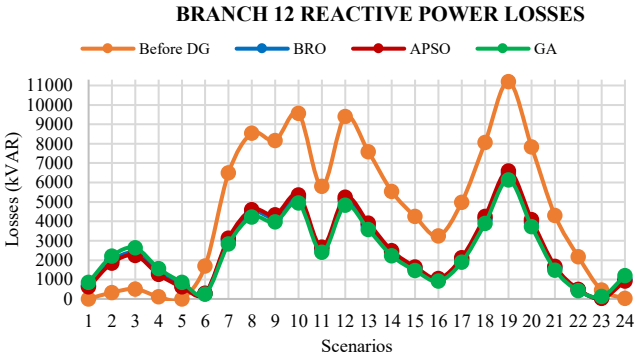

(l)

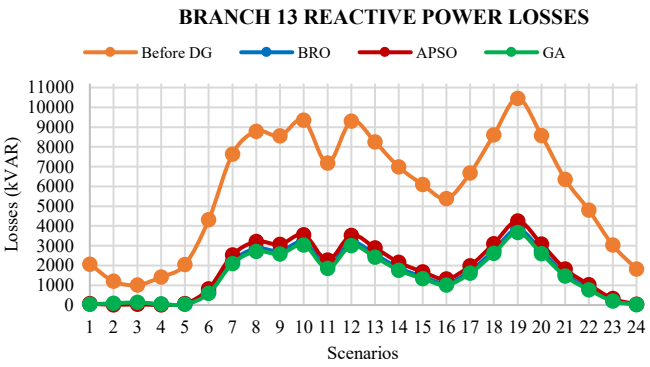

(m)

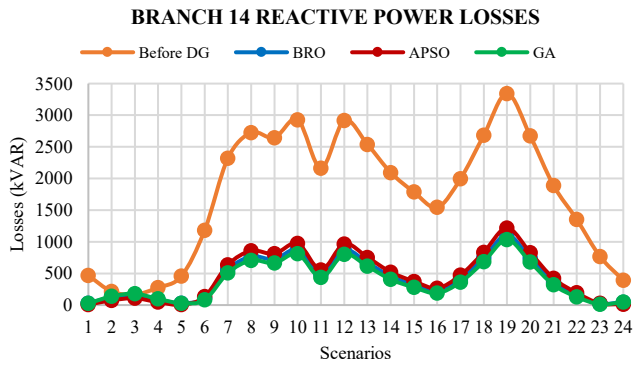

(n)

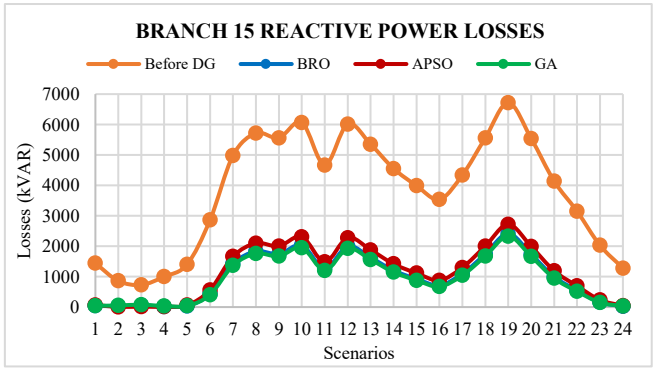

(o)

Figure 11. Reactive Power Losses of (a) Branch1, (b) Branch2, (c) Branch3, (d) Branch4, (e) Branch5, (f) Branch6, (g) Branch7, (h)Branch8, (i) Branch9, (j) Branch10, (k) Branch11 ,(l) Branch12, (m) Branch13, (n) Branch14, (0) Branch15

Preprints (www.preprints.org) | NOT PEER-REVIEWED | Posted: 6 May 2022 doi:10.20944/preprints202205.0057.v1

5.4. Bus Voltage Profiles

Voltage curves of buses for all scenarios of the existing system are shown in Figure 12. A summary of these results is also incorporated in Table 6, whereas the average voltages of all buses are illustrated in Table 9. After the placement of DGs for all scenarios, the voltage curves of bus 3 to bus 14 are shown in Figure 13. The voltage curves of bus1 and bus2 are not presented because of their negligible variations in all scenarios.

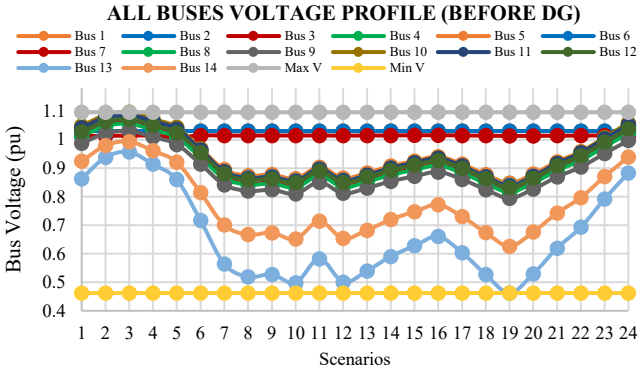

Figure 12. All Buses Voltage Profile (Before DG)

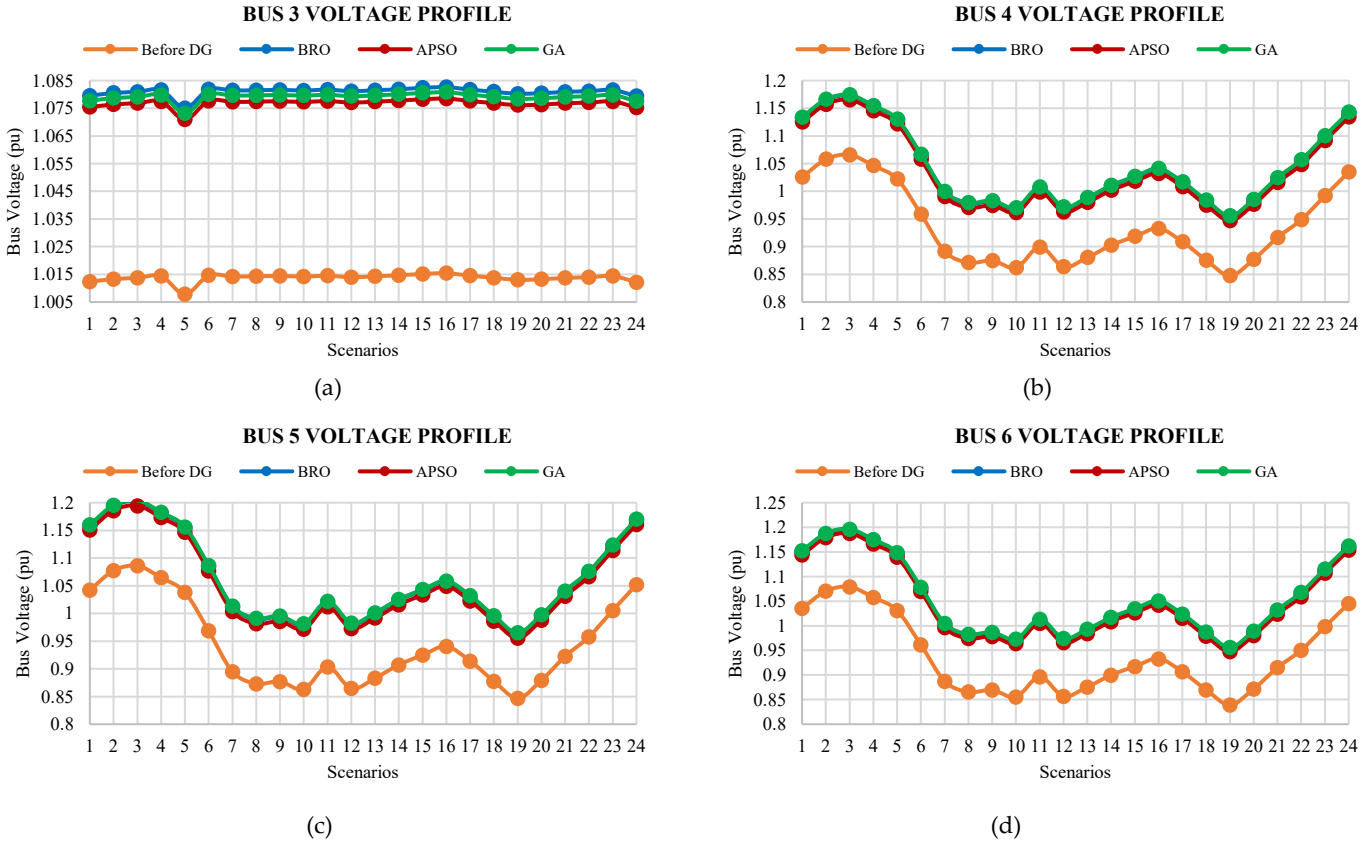

Table 9. Average Bus Voltages

Algorithms	Bus1	Bus2	Bus3	Bus4	Bus5	Bus6	Bus7	Bus8	Bus9	Bus10	Bus11	Bus12	Bus13	Bus14
Before DG	1.0300	1.0300	1.0138	0.9365	0.9444	0.9370	0.9168	0.9137	0.8906	0.9403	0.9389	0.9302	0.6654	0.7762
GA	1.0300	1.0300	1.0797	1.0447	1.0626	1.0554	1.0353	1.0322	1.0088	1.0712	1.0629	1.0488	0.9358	0.9735
APSO	1.0300	1.0300	1.0768	1.0359	1.0530	1.0458	1.0259	1.0227	0.9990	1.0605	1.0527	1.0391	0.9088	0.9545
Proposed BRO	1.0300	1.0300	1.0770	1.0434	1.0612	1.0539	1.0340	1.0309	1.0073	1.0696	1.0613	1.0473	0.9293	0.9699

Preprints (www.preprints.org) | NOT PEER-REVIEWED | Posted: 6 May 2022 doi:10.20944/preprints202205.0057.v1

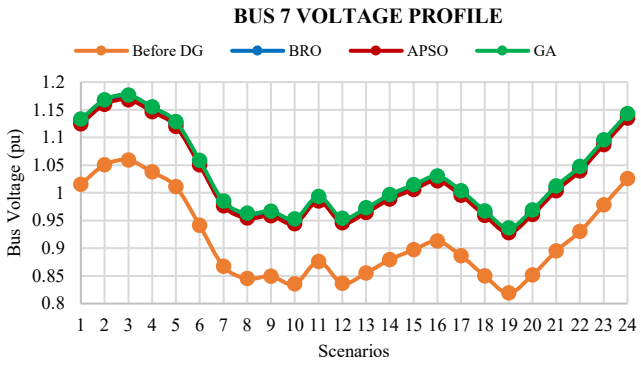

(e)

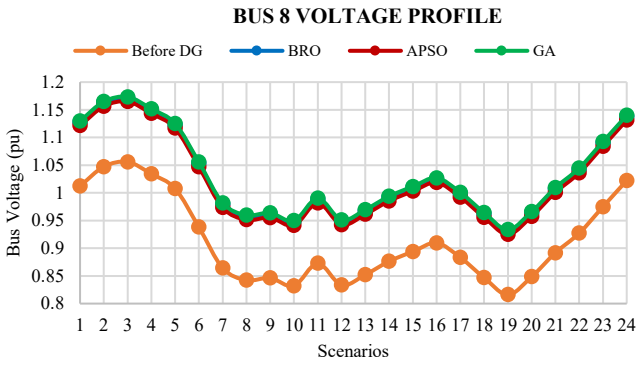

(f)

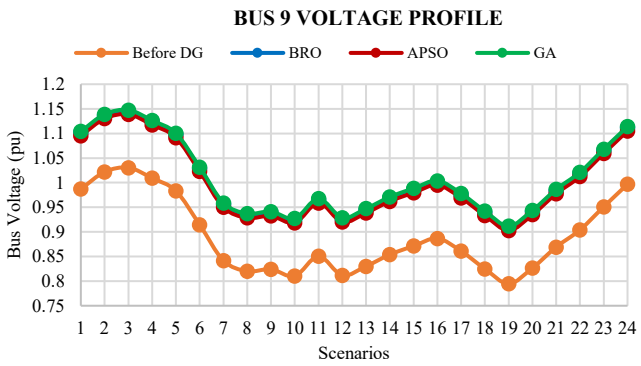

(g)

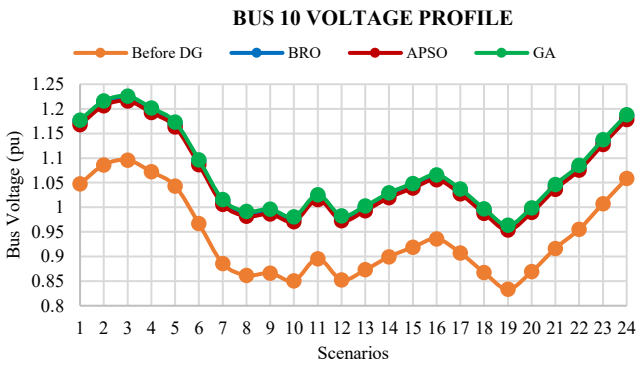

(h)

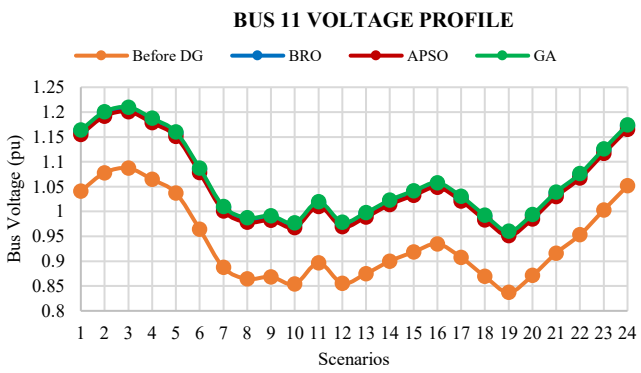

(i)

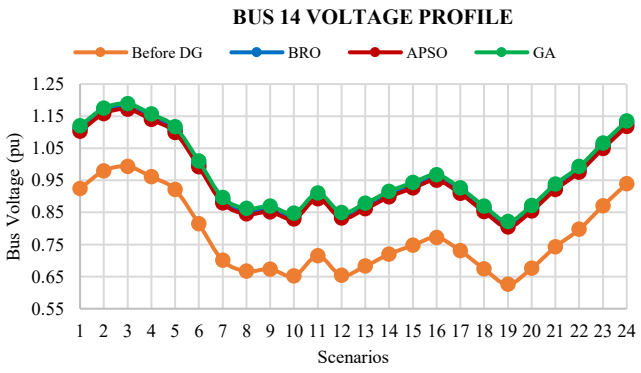

(j)

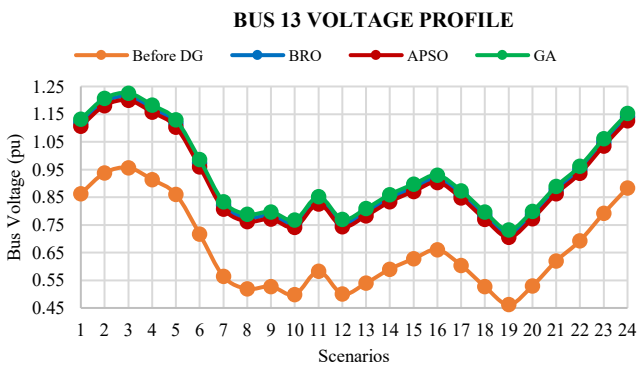

(k)

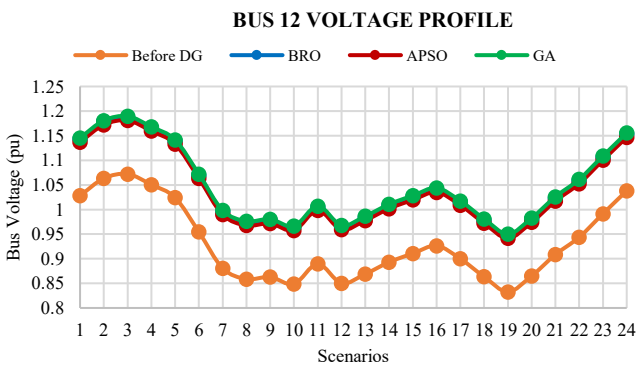

(l)

Figure 12. Votage Profiles of (a) Bus3, (b) Bus4, (c) Bus5, (d) Bus6, (e) Bus7, (f) Bus8, (g) Bus9, (h)Bus10, (i) Bus11, (j) Bus12, (k) Bus13 ,(l) Bus14

 doi:10.20944/preprints202205.0057.v1

6. Discussion

5.1. Active Power Losses

The results from Section 5 demonstrate appealing features of the designed methodology. Active power losses are analyzed in two ways, i.e., active power losses occurring at the overall system and active power losses occurring at each branch of the system. Following results are deduced after analyzing the active power losses of the system by using the designed methodology.

- Figure 8 and Table 6 depict the maximum active power loss that is 51604.96kW that occurs in the 19th scenario. This loss is minimized to 25471.47kW, 23123.32kW, and 22925.5kW by optimally allocating DGs via the usage of APSO, BRO, and GA algorithms.
- The Average active power loss arise at the existing system is 26617.93 kW along with all scenarios, which is reduced up to 11743kW, 12502.73kW, and 11794.14 kW using GA, APSO, and BRO algorithms, respectively.
- The existing active power loss from scenarios 2 to 4 are lesser than the losses calculated after the placement of DGs. Hence, the results described above signifies that the proposed method, when applied to allocate DGs in the system, aids in reducing the overall total active and reactive power losses in the system for all considered scenarios. Therefore, the planned DGs are delivering the same active power for a whole day. However, the power demand for scenarios 2 to 4 is lesser than the generated power, and it causes an increase in active power losses.
- The total active power losses for all scenarios are considered as active energy losses of 24 hours. After placement of DGs optimally, the active energy losses are calculated as 300065.4kWh, 281838kWh, and 283059.7kWh for APSO, GA, and BRO, respectively. Hence, it shows that 53.03%, 55.88%, and 55.69% of reduction in active energy loss has been seen in the system compared to the actual energy loss before the placement of DGs.
- Figure 9 elucidates that the active power losses are lower for most branches' initial and last scenarios. These scenarios incorporate off-peak hours, including late-night hours in which load requirement is lower than peak hours that are daytime. Therefore, the system losses are lower during the late-night period.
- The maximum loss occurs in the 19th scenario at most of the branches. The actual peak active power loss of 14569.43kW occurs among all branches of the system. This loss is minimized to 6619.197kW, 7199.756kW, and 6465.435kW by the optimal allocation of DGs using GA, APSO, and BRO cases, respectively.
- The actual minimum loss of 0.346432kW occurred among all branches of the system is further increased up to 1.392466kW, 1.45kW, and 1.384796kW while placing DGs using GA, APSO, and BRO algorithms, respectively.

5.2. Reactive Power Losses

Reactive power losses are analyzed in two ways, i.e., reactive power losses occurring at the overall system and reactive power loss occurring at each branch of the system. The main analysis of the outcome after analyzing the reactive power losses of the system is mentioned here under;

- Figure 10 and Table 6 show that the maximum reactive power loss is 53490.16kVAR which occurs for the 19th scenario. This loss is minimized up to 28191.04kVAR, 25669.27kVAR, and 25836.27kVAR, after the incursion of DGs in the system by using the APSO, BRO, and GA.
- The actual average reactive power loss for all scenarios is 26805.49kVAR. This loss is minimized up to 14412.65kVAR, 13813.92kVAR, and 13999.75kVAR, after the placement of DGs by using the APSO, BRO, and GA. It shows that the BRO has a better performance in the case of reactive power loss minimization.

Preprints (www.preprints.org) | NOT PEER-REVIEWED | Posted: 6 May 2022 doi:10.20944/preprints202205.0057.v1

- The present system's reactive power losses from scenarios 1 to 5 are lesser than the existing system before the placement of DGs. The proposed method is applied to allocate the optimal size and location of DGs while reducing the system's overall total reactive power losses for all considered scenarios. Therefore, the planned DGs are delivering the same power for a whole day. However, the power demand from scenarios 1 to 5 is lesser than the generated power and which has caused the increase in loss.
- The total reactive power losses for all scenarios are considered as reactive energy losses of 24 hours. After the placement of DGs, reactive energy losses are to be found as 345903.6 kVARh, 335994.1kVARh, and 331534.010kVARh by using APSO, GA, and BRO, respectively.
- The actual peak loss of 16907.7kVAR arises at branches is minimized to 9493.322kVAR, 10325.97 kVAR, and 9272.794kVAR by using GA, APSO, and BRO.
- The actual minimum loss of 0.498524 kVAR at branches is increased up to 1.98112 kVAR, 2.074574 kVAR, and 1.992093 kVAR by the usage of GA, APSO, and BRO.
- Figure 11 shows that reactive power losses for initial and last scenarios are lower. These scenarios represent late-night hours, and their load requirement is lower compared to daytime hours. Accordingly, the system losses are lower during the late-night period.
- The maximum reactive power loss arises for the 19th scenario at most branches. The maximum average reactive power loss occurs at branch 3. This loss is best minimized to 3811 kVAR by using the BRO.
- The average reactive power losses across branches 3, 5, 7, 12, and 13 are also best minimized by using the BRO.
- The average reactive power losses across branches 1, 2, 4, 6, 9, 10, and 11 are best minimized by using the APSO.
- The GA attains a better reactive power losses minimization for branches 8, 14, and 15.
- For busses 2, 4, 8, 9, 10, and 11, the average reactive power losses are increased after the placement of DGs.

5.3. Bus Voltage Profiles

The following analysis has been devised while studying bus voltage profiles.

- Figure 12 and Table 6 show that the actual minimum voltage across all buses is 0.4621pu. It has raised up to 0.726061pu, 0.705585pu, and 0.732564pu by individually using BRO, APSO, and GA.
- The maximum voltage before allocation of DGs is 1.0958pu which has enhanced up to 1.225032pu, 1.215942pu, and 1.226702pu by using the BRO, APSO, and GA.
- Figure 13 shows that the proposed method improves bus voltage profiles for all scenarios. The proposed BRO algorithm attains better performance in terms of voltage profile improvement as compare to the ASPO and GA.
- The average minimum voltage before placement of DGs is 0.6654pu at bus 13, which is improved to 0.9358pu, 0.9088pu, and 0.9293pu by using the GA, APSO, and BRO.

5.4. Main Findings and Comparison of Algorithms

MO, Maximum fitness, and other results are discussed in detail. Summary of main findings and comparison among BRO, APSO, and GA is presented in Table 6. The convergence curve of APSO, BRO, and GA is shown in Figure 6, which shows that APSO has best convergence among all three, BRO stands at second while GA has slowest convergence curve among all three. For the first time, the current work enlightened BRO algorithms for DGs' allocation. Figure 7 shows the comparison of convergence of APSO, BRO, and GA. Hence, APSO outperforms in attaining the least values of MO. The maximum

 doi:10.20944/preprints202205.0057.v1

fitness values of APSO, GA, and BRO, are 6.39, 6.69, and 6.48 respectively. This shows that APSO has least maximum fitness value. The performance of the GA is better than the BRO in terms of Maximum fitness, Vmin, Vmax, and total active power losses (active energy losses) as (ref Table 6). On the other hand, the BRO secures better outcomes in minimum and maximum branch losses (active and reactive) and total reactive power losses (reactive energy losses).

6. Conclusion

This paper exhibits an original work on optimal DGs allocation for the 24-hour load profile by using the min-max regret criteria. The study is conducted while considering the supplied power fluctuations in the renewable energy-based DGs. The performance is tested by using the CIGRE benchmark model. 24 scenarios are designed for studying specific load and generation profiles during the day hours. For each scenario, DGs' sizes and locations are determined on behalf of minimum MO values. Onward, a robust DGs allocation is determined for all scenarios on account of min-max regret criteria. Results achieved are promising and further shows validation of the minimization of total system losses, and bus voltage profiles are significantly improved by using the devised method. The BRO algorithm is first time implemented for optimal DGs allocation.

The maximum active and reactive line losses in the actual system are respectively 14569.43 kW and 16907.7 kVAR. These are minimized to 6465.435 kW and 9272.794 kVAR by using BRO. The maximum losses reduction obtained with GA are respectively 6619.197 kW and 9493.322 kVAR. In case of APSO, maximum line losses are lessened to 7199.756 kW and 10325.97 kVAR. The minimum actual busses voltages for all scenarios, are increased up to 0.726061 pu, 0.732564 pu and 0.705585 pu respectively by using BRO, GA and APSO. The system results show that the total active energy losses (active power losses for all scenarios) are minimized up to 55.69%, 55.88% and 53.03% using BRO, GA and APSO algorithms respectively for all scenarios. The reactive energy losses of the system (reactive power losses for all scenarios) are reduced up to 48.47%, 47.77% and 46.23% using BRO, GA and APSO algorithms respectively.

It confirms that the proposed BRO-based DGs deployment outperforms in terms of the system reactive power losses compared to GA and APSO-based deployment. Moreover, the busses voltage profile improvement obtained by BRO provided better results as compared to the results obtained from GA and APSO. The aforementioned outcomes achieved by using the proposed technique affirms the potential of integrating the proposed BRO-based DGs deployment approach in contemporary smart grids. The losses in few branches have been found to be increased by using the suggested method. A study on the minimization of this impact is in progress.

In the future, a battery storage system can also be introduced, and a detailed analysis of system faults and stability must be studied at multi-points. The incorporation of different types of hybrid DGs can improve a system's stability while minimizing its losses. Investigating this point is another future research axis.

Author Contributions: Conceptualization, A.A., S.M.Q. and A.W.; methodology, A.A and A.W.; implementation, A.A.; Validation, S.M.Q. and A.W.; formal analysis, N.U. and A.A.A.-A.; investigation, A.A., S.M.Q., A.W. and N.U.; resources, A.W. and A.A.A.-A.; writing—original draft preparation, A.A., S.M.Q. and A.W.; writing—review and editing, A.W., A.A.A.-A, and N.U.; visualization, A.A, S.M.Q, and A.W.; supervision, A.W. N.U. and A.A.A.-A; project administration, S.M.Q., A.W. and A.A.A.-A; funding acquisition, A.A.A.-A. All authors have read and agreed to the submitted version of the manuscript.

Funding: This research work is supported by Taif University Researchers Supporting Project number (TURSP-2020/121), Taif University, Taif, Saudi Arabia.

Institutional Review Board Statement: Not applicable.

Informed Consent Statement: Not applicable.

Data Availability Statement: Not applicable.

Ethical Approval: This article does not contain any studies with human participants or animals performed by any of the authors.

Acknowledgments: The research is technically supported by Bahria University under HEC's NRPU (20-14578/NRPU/R&D/HEC/2021).The authors acknowledge the financial support from Taif University Researchers Supporting Project Number (TURSP-2020/121), Taif University, Saudi Arabia.

Conflicts of Interest: Authors declare no conflict of interest.

References

1. Zohuri, Bahman, "Electricity, an Essential Necessity in Our Life," in Application of Compact Heat Exchangers For Combined Cycle Driven Efficiency In Next Generation Nuclear Power Plants, Springer Publishing, 2015, pp. 17-35.
2. M. F. N. Khan, T. N. Malik and I. A. Sajjad, "Impact of time varying load models on PV DG planning," Journal of Renewable and Sustainable Energy , vol. 10, no. 3, 2018.
3. Subhodip Saha and Vivekananda Mukherjee, "Optimal placement and sizing of DGs in RDS using chaos embedded SOS algorithm," IET Generation, Transmission & Distribution, vol. 10, no. 14, pp. 3671-3680, 2016.
4. Sajjan Kumar, Kamal K. Mandal and Niladri Chakraborty, "Optimal DG placement by multi-objective opposition based chaotic differential evolution for techno-economic analysis," Applied Soft Computing Journal, vol. 78, pp. 70-83, 2019.
5. Asad Waqar, Umashankar Subramaniam, Kiran Farzana and Rajavikram Madurai Elavarasan, "Analysis of Optimal Deployment of Several DGs in Distribution Networks Using Plant Propagation Algorithm," IEEE Access, vol. 8, pp. 175546 - 175562, September 2020.
6. Shamte Kawambwa, Ndyetabura Hamisi, Prosper Mafole and Helard Kundaeli , "A cloud model based symbiotic organism search algorithm for DG allocation in radial distribution network," *Evolutionary Intelligence,* p. 545–562, 2022.
7. Waseem Haider, S Jarjees Ul Hassan, Arif Mehdi and Arif Hussain, "Voltage Profile Enhancement and Loss Minimization Using Optimal Placement and Sizing of Distributed Generation in Reconfigured Network," *Machines,* 2021.
8. Mian Rizwan, Muhammad Waseem, Rehan Liaqat and Intisar Ali Sajjad, "SPSO Based Optimal Integration of DGs in Local Distribution Systems under Extreme Load Growth for Smart Cities," *Electronics,* 2021.
9. D. Nageswari, N. Kalaiarasi and G. Geethamahalaks, "Optimal Placement and Sizing of Distributed Generation Using Metaheuristic Algorithm," *Computer Systems Science and Engineering,* 2021.
10. Korra Balu and V. Mukherjee, "Optimal siting and sizing of distributed generation in radial distribution system using a novel student psychology-based optimization algorithm," *Neural Computing and Applications,* p. 15639–15667, 2021
11. Subrat Kumar Dash, Sivkumar Mishra, Almoataz Y. Abdelaziz, Mamdouh L. Alghaythi and Ahmed Allehyani, "Optimal Allocation of Distributed Generators in Active Distribution Networks Using a New Oppositional Hybrid Sine Cosine Muted Differential Evolution Algorithm," *Energies,* 2022.
12. M. I. Akbar, S. A. A. Kazmi, O. Alrumayh, Z. A. Khan, A. Altamimi and M. M. Malik, "A Novel Hybrid Optimization-Based Algorithm for the Single and Multi-Objective Achievement With Optimal DG Allocations in Distribution Networks," *IEEE Access,* vol. 10, pp. 25669 - 25687, 2022.
13. D.B.Prakash and C.Lakshminarayana, "Multiple DG placements in radial distribution system for multi objectives using Whale Optimization Algorithm," Alexandria Engineering Journal, vol. 57, no. 4, pp. 2797-2806, 2018.
14. S. H. Lee and J.-W. P. , "Optimal Placement and Sizing of Multiple DGs in a Practical Distribution System by Considering Power Loss," IEEE Transactions on Industry Applications (Volume: 49, Issue: 5, Sept.-Oct. 2013), vol. 49, no. 5, pp. 2262 - 2270, 2013.
15. M.A. Abdelkader, M.A. Elshahed and Z.H. Osman, "An analytical formula for multiple DGs allocations to reduce distribution system losses," Alexandria Engineering Journal, vol. 58, no. 4, pp. 1265-1280, December 2019.
16. M. F. N. Khan and T. N. Malik, "Probablistic generation model for optimal allocation of PV DG in distribution system," Journal of Renewable and Sustainable Energy, 2017.
17. A. Eid, "Allocation of distributed generations in radial distribution systems using adaptive PSO and modified GSA multi-objective optimizations," Alexandria Engineering Journal, vol. 59, no. 6, pp. 4771-4786, December 2020.
18. A. Ahmed, M. F. Nadeem and I. Ali, "Probabilistic generation model for optimal allocation of wind DG in distribution systems with time variable models," Sustainable Energy, Grids and Networks, vol. 22, May 2020.
19. Essam A.Al-Ammar, Kiran Farzana and Asad Waqar, "ABC algorithm based optimal sizing and placement of DGs in distribution networks considering multiple objectives," Ain Shams Engineering Journal, June 2020.
20. Minh-Thang Do, Antoine Bruyere and Bruno Francois, "Sensitivity analysis of the CIGRE distribution network benchmark according to the large scale connection of renewable energy generators," in 2017 IEEE Manchester PowerTech, Manchester, UK, 2017.

21. D. Rama Prabha and T. Jayabarathi, "Optimal placement and sizing of multiple distributed generating units in distribution networks by invasive weed optimization algorithm," Ain Shams Engineering Journal, vol. 7, no. 2, pp. 683-694, june 2016.
22. Aashish Kumar Bohre, Ganga Agnihotri and Manisha Du, "Optimal sizing and sitting of DG with load models using soft computing techniques in practical distribution system," IET Generation, Transmission & Distribution, vol. 10, no. 4, pp. 2606 - 2621, August 2016.
23. NaveenJain, S.N.Singh and S.C.Srivastava, "PSO based placement of multiple wind DGs and capacitors utilizing probabilistic load flow model," Swarm and Evolutionary Computation, vol. 19, pp. 15-24, 2014.
24. Arun Onlam, Daranpob Yodphet, Rongrit Chattha, Chayada Surawanitkun, Apirat Siritaratiwat and Pirat Khunkitti, "Power Loss Minimization and Voltage Stability Improvement in Electrical Distribution System via Network Reconfiguration and Distributed Generation Placement Using Novel Adaptive Shuffled Frogs Leaping Algorithm," Energies, 2019.
25. Ram Prakash, Ram Prakash and S. Sivasubramani, "Optimal Site and Size of DG with different Load Models using Cuckoo Search Algorithm," in 2018 IEEE International Conference on Power Electronics, Drives and Energy Systems (PEDES), Chennai, India, India, 2018.
26. Arulraj R and Kumarappan N, "Simultaneous Multiple DG and Capacitor Installation Using Dragonfly Algorithm for Loss Reduction and Loadability Improvement in Distribution System," in 2018 International Conference on Power, Energy, Control and Transmission Systems (ICPECTS), Chennai, India, 2018.
27. A. Dubey, "LOAD FLOW ANALYSIS OF POWER SYSTEMS," International Journal of Scientific & Engineering Research, vol. 7, no. 5, May-2016.
28. J.-H. Teng, "A modified Gauss-Seidel algorithm of three-phase power flow analysis in distribution networks," Int. J. Electr. Power Energy Syst., vol. 24, pp. pp. 97-102, , Feb. 2002.
29. T. R. Farshi, "Battle royale optimization algorithm," Neural Computing and Applications, May 2020.
30. X.-S. Yang, Engineering Optimization: an Introduction with Metaheuristic Applications, Hoboken, New Jersey: John Wiley & Sons, Inc, 2010.
31. Kumar Mahesh, Perumal AL Nallagownden and Irraivan AL Elamvazuthi, "Optimal placement and sizing of DG in distribution system using accelerated PSO for power loss minimization," in *2015 IEEE Conference on Energy Conversion*, Johor Bahru, Malaysia , 2016.
32. K.Prajna, G.Sasi Bhushan Rao and K.V.V.S.Reddy, "A New Dual Channel Speech Enhancement Approach Based on Accelerated Particle Swarm Optimization (APSO)," International Journal of Intelligent Systems Technologies and Applications, 2014.
33. Pandian Vasant, Jose Antonio Marmolejo, Igor Litvinchev and Roman Rodriguez Aguilar, "Nature-inspired meta-heuristics approaches for charging plug-in hybrid electric vehicle," Wireless Networks, p. 4753–4766, 2020.
34. Vijay Kumar Verma1 and Biresh Kumar, "Genetic algorithm: an overview and its application," International Journal of Advanced Studies in Computer Science and Engineering, vol. 2, no. 3, 2014.
35. M. Madhusudhan, N. Kumar and H. Pradeepa, "Optimal location and capacity of DG systems in distribution network using genetic algorithm," *International Journal of Information Technology*, p. 155–162, 2020.
36. Annu Lambora, Kunal Gupta and Kriti Chopra, "Genetic Algorithm- A Literature Review," in 2019 International Conference on Machine Learning, Big Data, Cloud and Parallel Computing (COMITCon), Faridabad, India, 2019.
37. Hassene Aissi, Cristina Bazgan and Daniel Vanderpooten, "Min–max and min–max regret versions of combinatorial optimization: A survey," European Journal of Operational Research, vol. 197, no. 2, p. 427–438, September 2009.
38. Mana Farrokhseresht, Han Slootweg and Madeleine Gibescu, "Day-ahead bidding strategies of a distribution market operator in a coupled local and central market," Smart Energy, vol. 2, 2021.
39. K. Rudion, A. O. and Z. S. , "Design of benchmark of medium voltage distribution network for investigation of DG integration," in 2006 IEEE Power Engineering Society General Meeting, Montreal, Que., Canada, 18-22 June 2006.
40. Strunz, K. & Abbasi, Ehsan & Fletcher, Robert & Hatziargyriou, Nikos & Iravani, Reza & Joos, Géza. (2014). TF C6.04.02 : TB 575 -- Benchmark Systems for Network Integration of Renewable and Distributed Energy Resources.
41. H. Liu, Y. J. and H. Z. , "Multi-Objective Dynamic Economic Dispatch of Microgrid Systems Including Vehicle-to-Grid," Energies, vol. 8, no. 5, pp. 4476-4495, 2015.

Appendix A

Table A1. Active Power Loads (kW)

Time (Hrs.)	Bus1 (kW)	Bus2 (kW)	Bus3 (kW)	Bus4 (kW)	Bus5 (kW)	Bus6 (kW)	Bus7 (kW)	Bus8 (kW)	Bus9 (kW)	Bus10 (kW)	Bus11 (kW)	Bus12 (kW)	Bus13 (kW)	Bus14 (kW)
1	5477.40	0.00	146.86	110.61	186.42	140.44	25.82	150.38	193.64	144.75	84.51	5535.11	11.48	165.32
2	5979.11	0.00	154.41	126.80	213.70	160.99	24.86	172.39	186.47	161.72	96.88	6034.69	11.05	169.00
3	4072.67	0.00	111.79	79.59	134.13	101.05	20.66	108.20	154.91	105.99	60.81	4118.84	9.18	127.96
4	3595.82	0.00	90.93	78.24	131.86	99.33	13.87	106.37	103.99	98.47	59.78	3626.81	6.16	97.88
5	4597.97	0.00	134.90	80.93	136.41	102.76	28.21	110.03	211.57	114.19	61.84	4661.03	12.54	161.34
6	5909.31	0.00	173.52	103.87	175.06	131.88	36.34	141.21	272.53	146.67	79.36	5990.53	16.15	207.65
7	9490.97	0.00	265.10	180.75	304.64	229.50	50.72	245.74	380.40	244.12	138.10	9604.35	22.54	307.12
8	13296.34	0.00	365.78	258.99	436.50	328.83	67.89	352.11	509.20	345.53	197.88	13448.10	30.18	419.34
9	14403.68	0.00	401.49	275.18	463.78	349.38	76.50	374.12	573.75	371.00	210.25	14574.68	34.00	464.45
10	14187.40	0.00	395.38	271.13	456.96	344.24	75.31	368.62	564.79	365.49	207.16	14355.73	33.47	457.32
11	14935.67	0.00	410.45	291.36	491.06	369.93	76.02	396.12	570.16	388.40	222.62	15105.60	33.79	470.20
12	12840.91	0.00	344.61	258.99	436.50	328.83	60.70	352.11	455.27	339.14	197.88	12976.60	26.98	388.18
13	14914.63	0.00	387.12	314.30	529.71	399.05	63.11	427.30	473.34	402.18	240.14	15055.71	28.05	425.34
14	13909.77	0.00	373.27	280.57	472.88	356.23	65.74	381.45	493.07	367.38	214.37	14056.73	29.22	420.44
15	12629.51	0.00	349.24	244.15	411.49	309.99	65.50	331.94	491.27	327.07	186.54	12775.93	29.11	401.81
16	11659.24	0.00	333.05	214.48	361.48	272.31	66.46	291.59	498.45	295.24	163.87	11807.79	29.54	391.61
17	10841.01	0.00	309.47	199.64	336.47	253.47	61.68	271.42	462.59	274.65	152.53	10978.88	27.41	363.73
18	12347.42	0.00	303.26	277.88	468.33	352.81	42.55	377.79	319.15	343.80	212.31	12442.54	18.91	318.65
19	14323.99	0.00	332.06	342.62	577.45	435.02	38.25	465.81	286.88	411.27	261.78	14409.49	17.00	331.29
20	16001.41	0.00	357.46	396.58	668.39	503.52	35.14	539.17	263.57	467.92	303.00	16079.96	15.62	343.89
21	14305.18	0.00	320.67	353.41	595.64	448.72	32.03	480.48	240.26	417.63	270.02	14376.79	14.24	309.57
22	12028.67	0.00	275.30	291.36	491.06	369.93	30.12	396.12	225.91	347.60	222.62	12096.00	13.39	271.30
23	10175.30	0.00	236.45	242.80	409.22	308.28	27.49	330.10	206.19	291.79	185.51	10236.75	12.22	236.44
24	7669.13	0.00	188.29	172.66	291.00	219.22	26.39	234.74	197.94	213.58	131.92	7728.12	11.73	197.79

Table A2. Reactive Power Loads (kW)

Time (Hrs.)	Bus1 (kVAR)	Bus2 (kVAR)	Bus3 (kVAR)	Bus4 (kVAR)	Bus5 (kVAR)	Bus6 (kVAR)	Bus7 (kVAR)	Bus8 (kVAR)	Bus9 (kVAR)	Bus10 (kVAR)	Bus11 (kVAR)	Bus12 (kVAR)	Bus13 (kVAR)	Bus14 (kVAR)
1	5180.28	0.00	124.96	66.23	111.62	84.08	28.04	90.04	210.27	97.84	50.60	5233.01	12.46	153.49
2	5664.39	0.00	128.11	75.92	127.95	96.39	27.00	103.21	202.48	107.59	58.00	5715.17	12.00	153.67
3	3847.52	0.00	96.56	47.65	80.31	60.50	22.43	64.78	168.22	72.41	36.41	3889.71	9.97	120.21
4	3409.69	0.00	74.33	46.84	78.95	59.47	15.06	63.68	112.92	64.96	35.79	3438.01	6.69	87.88

 doi:10.20944/preprints202205.0057.v1

5	4329.62	0.00	121.23	48.46	81.67	61.52	30.63	65.88	229.74	80.59	37.02	4387.24	13.61	156.15
6	6974.13	0.00	156.01	62.19	104.81	78.96	39.46	84.55	295.94	103.55	47.51	5638.40	17.54	201.03
7	8958.81	0.00	231.48	108.22	182.40	137.40	55.08	147.13	413.07	168.12	82.69	9062.39	24.48	290.95
8	12559.96	0.00	316.39	155.06	261.34	196.88	73.73	210.82	552.94	236.28	118.48	12698.62	32.77	394.39
9	13597.42	0.00	350.11	164.75	277.68	209.18	83.07	223.99	623.03	255.26	125.88	13753.66	36.92	439.57
10	13393.39	0.00	344.74	162.33	273.59	206.11	81.77	220.70	613.29	251.43	124.03	13547.19	36.34	432.78
11	14109.20	0.00	354.79	174.45	294.01	221.49	82.55	237.17	619.13	265.46	133.28	14264.46	36.69	442.00
12	12143.84	0.00	293.40	155.06	261.34	196.88	65.92	210.82	494.37	229.34	118.48	12267.81	29.30	360.55
13	14126.40	0.00	322.31	188.18	317.15	238.92	68.53	255.83	514.00	268.12	143.77	14255.29	30.46	387.89
14	13154.72	0.00	317.78	167.98	283.12	213.28	71.39	228.38	535.41	248.43	128.35	13288.99	31.73	390.51
15	11927.13	0.00	303.06	146.18	246.37	185.60	71.13	198.74	533.47	224.19	111.69	12060.91	31.61	378.85
16	10993.47	0.00	294.73	128.41	216.42	163.04	72.17	174.58	541.25	205.55	98.11	11129.21	32.07	374.77
17	10222.30	0.00	273.76	119.53	201.45	151.76	66.98	162.50	502.31	191.15	91.32	10348.27	29.77	347.98
18	11722.94	0.00	242.61	166.37	280.40	211.23	46.21	226.19	346.56	224.27	127.11	11809.84	20.54	280.61
19	13631.72	0.00	253.68	205.14	345.73	260.45	41.54	278.89	311.51	262.80	156.73	13709.84	18.46	279.10
20	15250.04	0.00	264.43	237.44	400.18	301.47	38.16	322.81	286.20	295.37	181.42	15321.82	16.96	280.08
21	13631.68	0.00	237.94	211.60	356.62	268.66	34.79	287.68	260.89	263.91	161.67	13697.10	15.46	252.97
22	11453.12	0.00	208.03	174.45	294.01	221.49	32.71	237.17	245.32	221.16	133.28	11514.64	14.54	226.02
23	9682.61	0.00	181.00	145.37	245.01	184.57	29.85	197.64	223.90	186.61	111.07	9738.75	13.27	199.60
24	7281.36	0.00	150.59	103.38	174.23	131.25	28.66	140.54	214.94	139.30	78.98	7335.26	12.74	174.14